MODULATION OF ALPHA-CRYSTALLIN-MEMBRANE ASSOCIATION BY PHOSPHOLIPID ACYL CHAIN LENGTH AND DEGREE OF UNSATURATION

by

Geraline Trossi-Torres

A thesis

submitted in partial fulfillment

of the requirements for the degree of

Master of Science in Biomolecular Sciences

Boise State University

December 2022

BOISE STATE UNIVERSITY GRADUATE COLLEGE

DEFENSE COMMITTEE AND FINAL READING APPROVALS

of the thesis submitted by

Geraline Trossi-Torres

Thesis Title: Modulation of Alpha-Crystallin-Membrane Association Modulated by Phospholipid Acyl Chain Length and Degree of Unsaturation

Date of Final Oral Examination: 03 October 2022

The following individuals read and discussed the thesis submitted by Geraline Trossi-Torres, and they evaluated the student's presentation and response to questions during the final oral examination. They found that the student passed the final oral examination.

Laxman Mainali, Ph.D.	Chair, Supervisory Committee
Henry A. Charlier, Jr., Ph.D.	Member, Supervisory Committee
Matthew L. Fergurson, Ph.D.	Member, Supervisory Committee

The final reading approval of the thesis was granted by Laxman Mainali, Ph.D., Chair of the Supervisory Committee. The thesis was approved by the Graduate College.

DEDICATION

I want to dedicate this thesis to my mother, father, brother, and sister for their immense support throughout this journey.

ACKNOWLEDGMENTS

I would like to express my deepest gratitude to my advisor, Dr. Laxman Mainali, for his guidance, patience, and feedback throughout this thesis journey. I would also like to thank my thesis committee members: Dr. Henry Charlier and Dr. Matthew Fergurson, for their immense support. Finally, I am incredibly grateful to the Bridge to Doctorate Fellowship for its tangible support and guidance throughout this endeavor.

I am also grateful to the postdoc fellows from my lab: Dr. Raju Timsina and Dr. Nawal Khadka, who generously provided their knowledge and expertise throughout this journey. Finally, I would like to extend my sincere thanks to the Biomolecular Sciences Program for their support throughout the thesis.

Lastly, I'd like to mention my family, especially my parents and siblings, for their unconditional emotional and moral support. Their belief in me through this endeavor has motivated me to continue going through this process, for which I am truly grateful.

ABSTRACT

Cataract is the leading cause of blindness worldwide. The only treatment for cataracts is the surgical removal of the cataractous lens and the replacement of an intraocular lens. With less availability of treatment and low income, the visual damage caused by cataracts can go untreated. The cataract may develop again after surgery, such as posterior capsule opacification. With age and cataracts, α-crystallin, a significant protein of the mammalian eye lens, is progressively associated with the eye lens membrane. The primary association sites of α-crystallin with the membranes are phospholipids. However, it is unclear if phospholipids' acyl chain length and degree of unsaturation influence the α-crystallin association. We used the electron paramagnetic resonance (EPR) approach to investigate the association of α-crystallin with phosphatidylcholine (PC) membranes of different acyl chain lengths and degrees of unsaturation, with and without cholesterol (Chol). The association constant (K_a) of α-crystallin follows the trends, i.e., K_a (14:0–14:0 PC) > K_a (18:0–18:1 PC) > K_a (18:1–18:1 PC) ≈ K_a (16:0–20:4 PC) where the presence of Chol decreases K_a for all membranes. With an increase in α-crystallin concentration, the saturated and monounsaturated membranes rapidly become more immobilized near the headgroup regions than the polyunsaturated membranes. Our results directly correlate the mobility and order near the headgroup regions of the membrane with the K_a, with the less mobile and more ordered membrane having substantially higher K_a. Furthermore, our results show that the hydrophobicity near the headgroup regions of the membrane increases with

the α-crystallin association, indicating that the α-crystallin-membrane association forms the hydrophobic barrier to the transport of polar and ionic molecules, supporting the barrier hypothesis in cataract development. Taken together, our findings clearly show how the changes in phospholipids' acyl chain length and degree of unsaturation influence α-crystallin association with model membranes and provide insight for further investigations to examine how such changes in lipids in the eye lens membranes with age and cataracts modulate α-crystallin association with native membranes.

TABLE OF CONTENTS

LIST OF FIGURES

Published Article Title: Alpha-Crystallin-Membrane Association Modulated by Phospholipid Acyl Chain Length and Degree of Unsaturation

Authors: Geraline Trossi-Torres[1], Raju Timsina[2] and Laxman Mainali[1,2*]

[1] Biomolecular Sciences Graduate Program, Boise State University, Boise, ID 83725, USA

[2] Department of Physics, Boise State University, Boise, ID 83725, USA

* Correspondence: laxmanmainali@boisestate.edu

Citation: Trossi-Torres, G.; Timsina, R.; Mainali, L. Alpha-Crystallin-Membrane Association Modulated by Phospholipid Acyl Chain Length and Degree of Unsaturation. Membranes 2022, 12, 455. https://doi.org/10.3390/membranes12050455

https://doi.org/10.3390/membranes12050455

https://www.mdpi.com/2077-0375/12/5/455

CHAPTER 1: OVERVIEW

Structure of the Human Eye

The human eye lens is composed of various sections, as shown in Figure 1. The sclera is the outermost layer of the human eye, which protects the eyeball. The transparent front part of the eye is the cornea, which functions to help focus the light onto the eye lens.[1] There is a choroid beneath the outermost layer where the iris is located, and the pupil controls the amount of incoming light.[1] Aqueous humor is a fluid in which the iris and lens are bathed. The aqueous humor fluid functions as a transparent circulatory system that controls the intraocular pressure, but it can also provide nutrition to the lens and cornea. It can also remove excess debris from other ocular tissues.[1] The eye lens is located behind the iris.

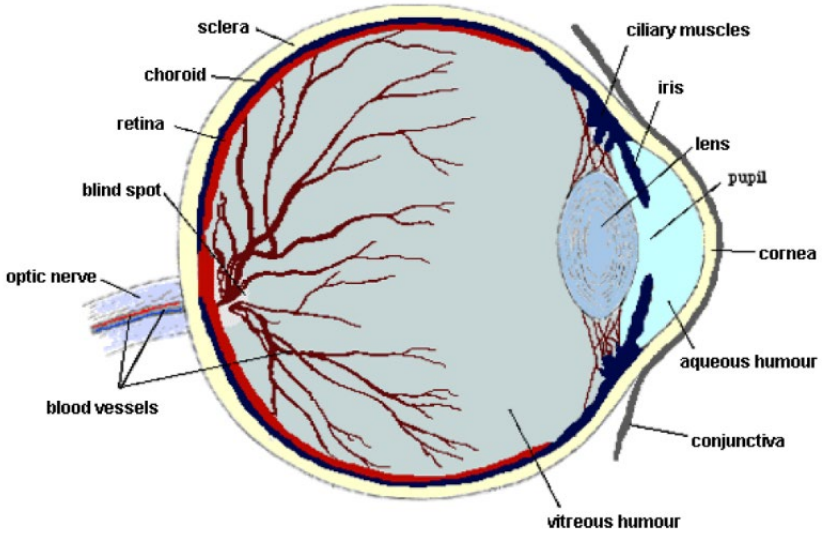

Figure 1 Structure of the Human Eye2

Structure of the Human Eye Lens

The eye lens is a transparent, biconvex structure in the eye that functions to focus incoming light onto the retina. The light refracted by the lens and focused onto the retina is shown in Figure 2. Figure 2A shows that the lens focuses parallel light rays from a distant object onto the retina. Figure 2B shows that the lens focuses the diverging light rays from the nearby object onto the retina. The shape of the eye lens changes, by changing the lens's focal length while focusing the light onto the retina, known as accommodation. The suspensory ligaments and ciliary muscles control the shape of the lens. For parallel light rays from a distant object, the eye lens becomes thin with suspensory ligaments tight, and the ciliary muscle relaxed, as shown in Figure 2A. For Diverging light rays from nearby objects, the eye lens becomes thick with suspensory ligaments loose and ciliary muscle contracted, as shown in Figure 2B. Most importantly, the eye lens should be transparent to focus light onto the retina. For the eye lens to be transparent, the lens is packed with highly specialized and tightly structured cells called fiber cells.

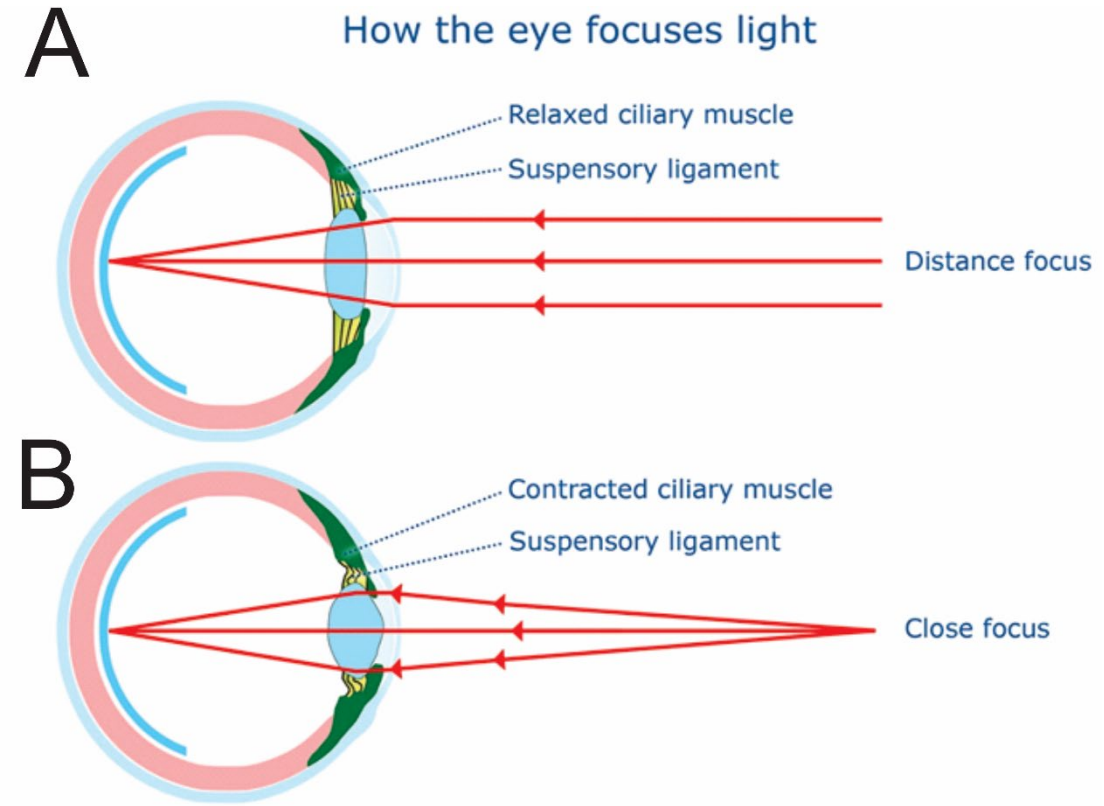

Figure 2 Refraction of Light onto Retina (A-B) Light is refracted by the lens and focused onto the retina. A) Lens focuses parallel light rays from a distant object onto the retina. B) Lens focuses the diverging light rays from the nearby object onto the retina.3

Figure 3 shows the arrangement of lens cells. The epithelium of the lens on the outer cortex creates the fiber cells. The mature fiber cells lose organelles and nuclei to become transparent. The lens membrane and cytoskeleton remain in the mature fiber cells as the supramolecular structure.[4,5] The younger fiber cells remain in the outer layers called the cortex, and the older fiber cells remain in the inner layers called the nucleus. The human eye lens grows from 65 mg at birth to 250 mg by the age of 90.[6,7] The lens fiber cells contain a large concentration of proteins such that approximately 60% of the mass of the eye lens is protein mass.[7] Approximately 90% of the proteins are crystallin proteins, namely α-, β-, and γ-crystallins.[8–10] The function of crystallins is to maintain the transparency and refractivity of the lens.[11] Out of three crystallins, α-crystallin accounts

for approximately 40% of the lens proteins[8,10] and functions as a molecular chaperone preventing the aggregation of other proteins and acting as a heat shock protein in the lens.[12,13] The crystallin proteins in the lens remain in the lens for the lifetime of species.[14] Therefore, α-crystallin's chaperon-like activity is highly significant for the lifetime transparency of the lens.

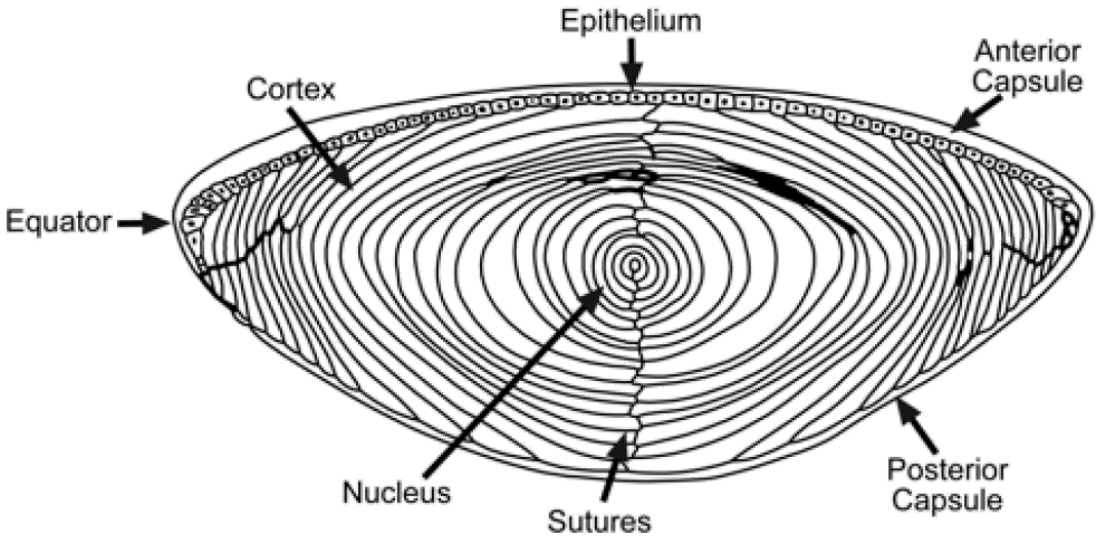

Figure 3 Structure of the Human Eye Lens2

The lens membranes consist of lipids (phospholipids (PL), sphingolipids (SLs), and cholesterol (Chol)) as well as integral membrane proteins. The lens membranes contain higher cholesterol content than any other body parts.[15]

Changes in the eye lens occur with age, with the lens becoming less transparent and stiffer. In addition, the lipid content changes, and lipids and crystallin proteins modify with age, which deteriorates the chaperon-like activity of α-crystallin, induces the accumulation of proteins in the lens, and the association of proteins with the lens membranes, negatively impacting the lens transparency.

Cataracts

Cataracts develop in the eye lens, which causes blurry and foggy vision, affecting half of Americans by age 80. One of the primary causes of cataract development is aging.[16–18] The standard lens focuses light onto the retina, but the cataractous lens scatters light instead of focusing onto the retina, as shown in Figure 4. Therefore, cataractous eyes produce blurry and foggy vision.

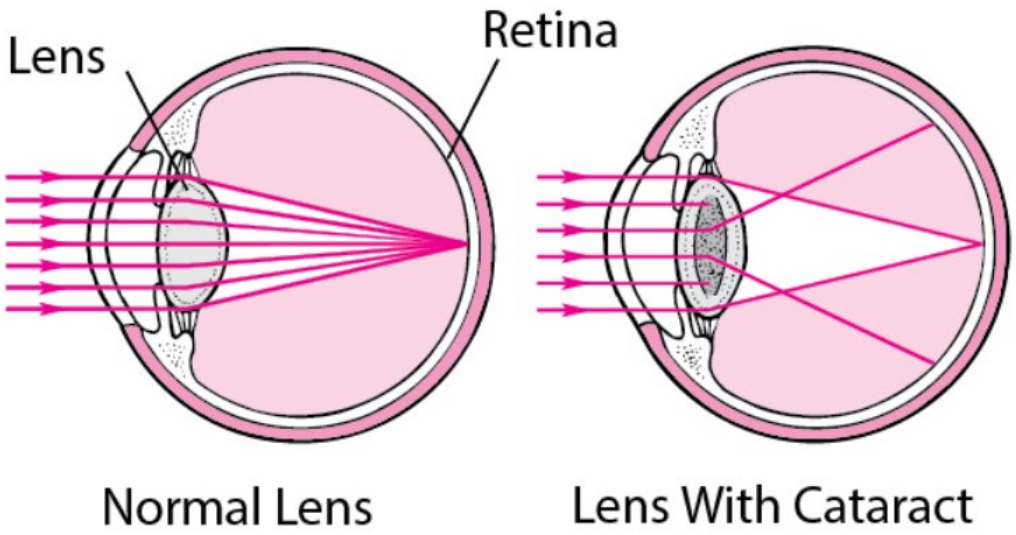

Figure 4 Difference between a healthy eye lens and an eye lens with cataracts. Healthy human eye lens (left). Cloud formation in the human eye lens produces light scattering that affects vision (right).19

Figure 5 shows the changes in the human lens due to age and cataracts. The clear middle lens in Figure 5 shows the clear human lens. The human lens clouds due to cataracts, as shown in the left top lens in Figure 5. The human lens becomes yellow with aging, as shown in the top right lens in Figure 5. The big bottom lens in Figure 5 shows the clear bovine lens.

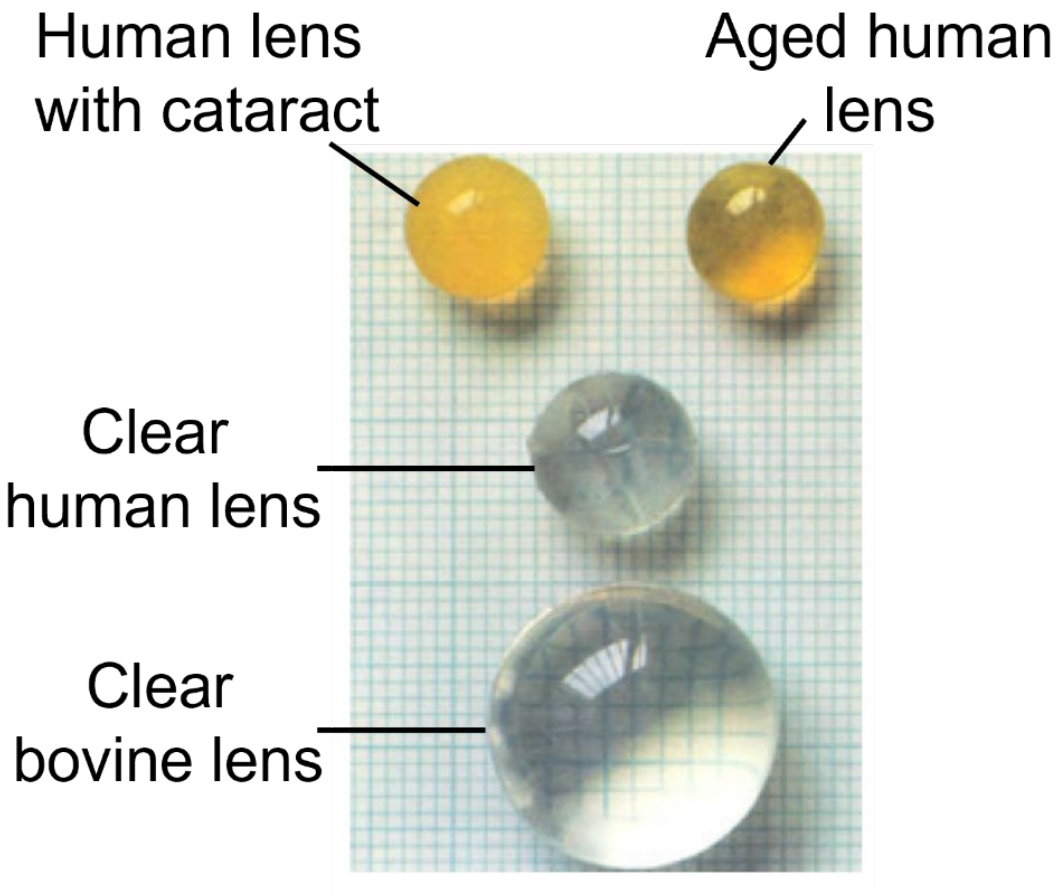

Figure 5 Changes in human eye lens due to age. Clear human eye lens (middle) to yellow eye lens due to aging (top right), cloudy eye lens due to cataract (top left), and cow eye lens (bottom).2

Lipids and proteins in the human eye lens change with aging. The lipids in the lens membrane may oxidize[20–25], and lipid composition changes[26–33] with age. Moreover, crystallin and integral membrane proteins may mutate[34–37], and post-translational modifications (PTM)[38,39,40–48] may occur in these proteins. Such changes in lipids and proteins induce the cataract, but the exact mechanism of how cataracts form are not fully understood.

Currently, cataracts are the leading cause of blindness globally. The only treatment for cataracts is surgery, in which the cataractous lens is removed with the insertion of the intraocular lens. In this procedure, the eye capsule remains intact, and

some epithelial cells remain there, which may grow and cause cataracts again, such as posterior capsule opacification (PCO). However, with less access to medical care and low income, cataract surgery may be impossible. Therefore, it would be very significant and beneficial if cataracts could be treated and cured without surgery. The understanding of the mechanism of cataract formation is, therefore, critical.

Cataract Formation and α-crystallin-Membrane Association

Aging is the most common cause of cataracts[49,50], but it may also develop due to radiation exposure[51–53], genetic factors[54,55], trauma[56,57], diseases (e.g., diabetes and hypertension)[58,59], etc. As shown in Figure 6, α-crystallin binds with the human eye lens membrane containing phospholipids, sphingolipids, cholesterol, integral membrane proteins such as aquaporin-0 (AQP0), and connexins.[60–63] α-crystallin-membrane association in the lens increases significantly with age[64–70], deteriorating α-crystallin's chaperone activity and contributing to cataract formation.[50,71] Clinical study shows that the level of α-crystallin in the eye lens cytoplasm decreases with age and cataract formation, with a corresponding increase in α-crystallin-membrane association, resulting in light scattering and cataract formation.[72] The primary association sites of α-crystallin in the lens membranes are the intrinsic phospholipids (PLs) and sphingolipids (SLs).[73–75] PLs and SLs have a hydrophilic "head" containing a phosphate group and two hydrophobic "tails" made of fatty acids. How PLs' fatty acid tails influence α- crystallin-membrane association is still unclear. This thesis research explores the unclear roles of PLs acyl chain length and degree of unsaturation on α-crystallin-membrane association using the model membranes made of phosphatidylcholine (PC), a dominant PL in the eye lens of lower-aged animals.[76]

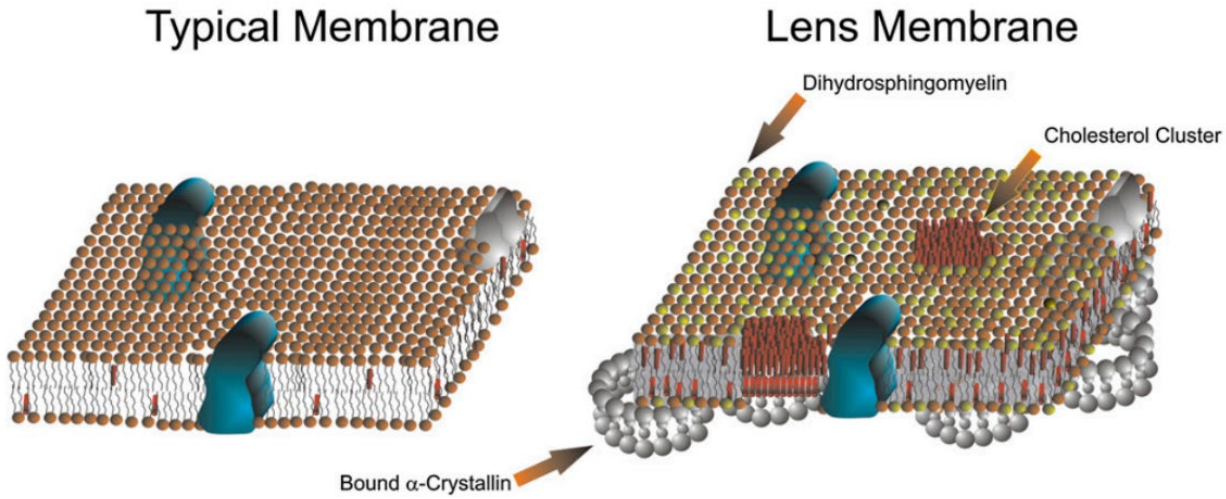

Figure 6 Typical membrane (left) and human eye lens membrane (right).17

Outline of Thesis

This thesis aims to understand how the α-crystallin-membrane association is modulated by the acyl chain length and degree of unsaturation of PLs in membranes, using a well-known electron paramagnetic resonance (EPR) spin-labeling method. Dramatic changes in lens lipid composition occur with age, with acyl chains of lipids becoming shorter and more saturated.[33,76–79] The PC is the dominant PL in the eye lens membranes of lower-aged animals.[76] My research focuses on the native bovine α-crystallin association with the model membranes made of PC with different acyl chain lengths and degrees of unsaturation. The EPR spin-labeling method was chosen because this method, developed in our laboratory, is well-suited to probe the association of α-crystallin with model and native lens membranes and the physical properties of the membranes, such as mobility parameter, maximum splitting, and hydrophobicity.

The research is motivated by the overview in Chapter 1. The introduction in Chapter 2 includes a literature review, briefly explaining the previous research on α-crystallin-membrane association. It also briefly explains previous research in our

laboratory and the inspiration for the research reported in this thesis. Chapter 3 includes the materials and methods. It explains how we prepare membrane samples, mixtures of α-crystallin and membrane samples, perform EPR experiments, and probe the α-crystallin association with membranes and the physical properties of the membranes. Chapter 4 includes results and discussion. We present the quantitative measurements of the percentage of membrane surface occupied by α-crystallin, binding affinity (K_a), and the physical properties of membranes (mobility parameter, maximum splitting, and hydrophobicity). We add ~23 mol% cholesterol (Chol), a significant component of the eye lens membrane, to the PC membranes and probe the role of Chol on α-crystallin association with PC membranes. The conclusion in Chapter 5 concludes this thesis. The data presented in this thesis work is published in the peer-reviewed journal Membranes.

CHAPTER 2: INTRODUCTION

Eye lens lipid composition changes dramatically with age, increasing the SL content[80–83] and saturation levels of PL acyl chains and decreasing the acyl chain length.[80–84] These changes in lipid composition are observed between the lens cortex and nucleus of clear lenses of different age groups and age-matched cataractous human lenses.[85–87] It has been speculated that, with an increase in lipid chain order of membrane with age and cataract[88–90], the association of α-crystallin with membrane might increase.[91] However, it is not clear whether the length of the acyl chain and degree of unsaturation influence the α-crystallin-membrane association. Very few studies have been performed earlier to investigate the role of acyl chain length and degree of unsaturation in α-crystallin membrane association, and the results are conflicting. For example, Cobb and Petrash[84] used AlexaFluor350TM-conjugated α-crystallin with different synthetic vesicles where vesicles were made of phosphatidylcholine (PC) with different chain lengths and degrees of unsaturation. They reported that acyl chain length and degree of unsaturation do not influence the association of α-crystallin to lipid membranes. However, Tang et al.[91] used the fluorophore NBD-PE to investigate the association of α-crystallin with distearoylphosphatidylcholine (DSPC), sphingomyelin (SM), and egg-phosphatidylcholine (egg-PC) membranes and found that the α-crystallin-membrane association depends on lipid chain order, with a more prominent association observed with ordered membranes. The association of α-crystallin with membranes alters the physical properties of membranes[18,91], possibly playing a significant role in modulating

the integrity of membranes. Borchman and Tang[92] used NBD-PE fluorophore, which resides near the lipid headgroup region, to investigate the physical properties of bovine lens lipid vesicles with the α-crystallin association and discovered that water is excluded from the lipid headgroup regions and headgroup mobility is reduced. It has also been reported that, during aging, lipid headgroup order is modulated in the human lens membrane with the association of α- and β-crystallin.[93] A hypothesis has been made that the association of α-crystallin to lens membrane contributes to nuclear cataract development by obstructing membrane pores and creating a diffusion barrier.[94–96] The transport of polar and ionic molecules between fiber cells in the lens is controlled by abundant integral membrane proteins aquaporin-0 (AQP0) and connexins (Cx46 and Cx50).[60,97,98] It has been reported that ionic imbalance in the lens could cause membrane swelling followed by loss of lens transparency.[99–101] The association of α-crystallin to the lens membrane may form the diffusion barrier resulting in the disruption of water and ion homeostasis in the lens. However, it is unclear whether changes in the physical properties of the membrane caused by the α-crystallin association create a diffusion barrier.

We used the EPR spin-labeling approach to investigate the association of α-crystallin with membranes made of individual lipids[102,103] and two-component lipid mixtures[103,104], where membranes had the same hydrophobic fatty acid core but different headgroups. Our results show that lipid headgroup size and charge, hydrogen bonding between lipid headgroups, and lipid curvature modulate α-crystallin-membrane association and the physical properties of membrane changes with α-crystallin association.[18,103–105] Moreover, our results show that, independently of the lipid headgroup, cholesterol (Chol) inhibits α-crystallin membrane association; however, the

inhibition level differed depending upon the lipid headgroup.[18,104,105] Cobb and Petrash et al.[106] showed that the R116C mutation in αA-crystallin decreased the chaperone-like activity and ability to exchange subunits by 4-fold and increased the αA R116C membrane association capacity by 10-fold, potentially being the cause of congenital cataracts. Srivastava et al.[101] showed that N101D deamidation in αA-crystallin increased association with the mice lens membrane, potentially causing intracellular ionic imbalance and membrane disorganization, successively leading to cortical cataracts. These studies[101,106] are based on the role of α-crystallin mutation and post-translational modification in α-crystallin-membrane association and cataracts.

The study reported in this thesis investigates the association of α-crystallin with cholesterol (Chol)/phosphatidylcholine (PC) membranes with different chain lengths and degrees of unsaturation (i.e., 1,2-dimyristoyl-sn-glycero-3-phosphocholine (DMPC; 14:0–14:0 PC), 1-stearoyl-2-oleoyl-sn-glycero-3-phosphocholine (SOPC, 18:0–18:1 PC), 1,2-dioleoyl-sn-glycero-3-phosphocholine (DOPC; 18:1–18:1 PC), and 1-palmitoyl-2-arachidonoyl-sn-glycero-3-phosphocholine (PAPC; 16:0–20:4 PC)) and in the presence and absence of 23 mol% Chol. The novelty of this study is that it investigates the role of membrane PLs' acyl chains by varying the lipid chain length and degree of unsaturation and probes the effect of such variation in the α-crystallin-membrane association. This research also illustrates the lipid chain length and degree of unsaturation in modulating the membranes' physical properties (maximum splitting, mobility parameter, and hydrophobicity) with the α-crystallin association. Furthermore, hydrophobicity measured near the membrane surface with α-crystallin association provides new insight into the

hydrophobic barrier on the lens membrane surface, supporting the barrier hypothesis in cataract development.

CHAPTER 3: MATERIALS AND METHODS

Materials

DMPC (14:0–14:0 PC), SOPC (18:0–18:1 PC), DOPC (18:1–18:1 PC), PAPC (16:0–20:4 PC), and Cholesterol (Chol) were purchased from Avanti Polar Lipids, Inc. (Alabaster, AL, USA). The cholesterol analog cholestane spin-label (CSL) and bovine eye lens α-crystallin were purchased from Sigma Aldrich (St. Louis, MO, USA), where α-crystallin was used without further purification. Based on the information (αA = 19.8 kDa, αB = 22 kDa, and αA:αB = 3:1), the average molecular weight for the α-crystallin subunit was estimated to be 20.35 kDa. Preparation of membranes, α-crystallin, and α-crystallin membrane association studies was performed in HEPES buffer (10 mM HEPES, 100 mM NaCl, pH = 7.4).

Sample Preparation for α-Crystallin-Membrane Association Studies

Phospholipids (PLs) of varying chain lengths and degrees of unsaturation have been chosen to prepare the membrane samples. Figure 7 shows the chemical structure of saturated PL (DMPC) with a short acyl chain length where both chains are saturated, i.e., 14:0–14:0 PC, monounsaturated PL (SOPC) where one acyl chain is saturated and another acyl chain contains one double bond, i.e., 18:0–18:1 PC, polyunsaturated PL (DOPC) where each acyl chain contains one double bond, i.e., 18:1–18:1 PC, and polyunsaturated PL (PAPC) where one acyl chain is saturated and another acyl chain contains four double bonds, i.e., 16:0–20:4 PC.

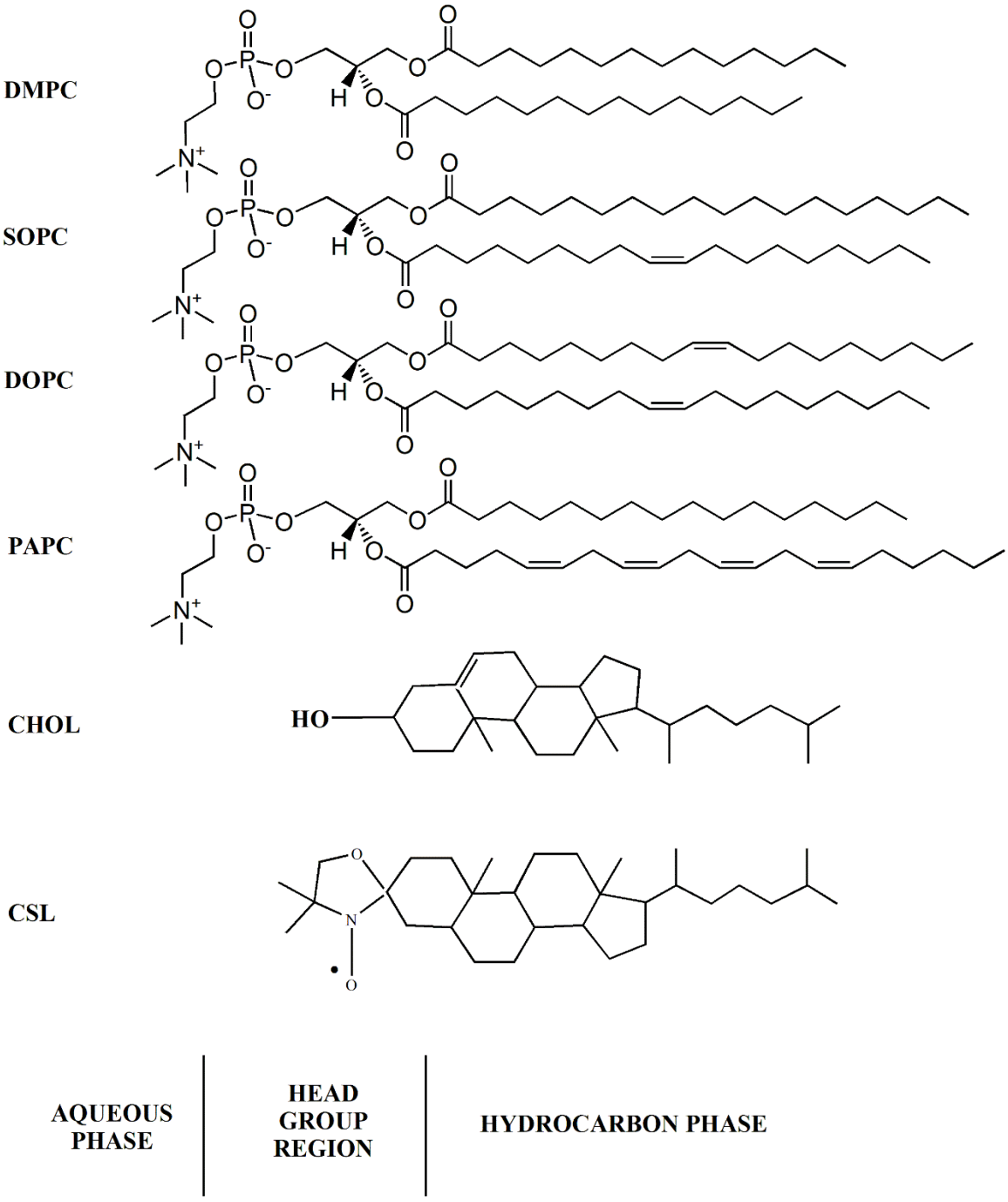

Figure 7 The chemical structure of 14:0-14:0 PC (DMPC), 18:0-18:1 PC (SOPC), 18:1-18:1 PC (DOPC), 16:0-20:4 PC (PAPC), cholesterol (Chol), and cholesterol analogue spin-label (CSL). The approximate locations of each molecule across the lipid bilayer membrane are indicated.

The chemical structure of Chol and CSL with the approximate locations in the PL bilayer membrane is shown in Figure 7. The nitroxide moiety of the CSL spin-label close

to the headgroup regions of the membranes, as shown in the schematic diagram in Figure 8, monitors the α-crystallin-membrane association, and the physical properties changed due to such association. The advantage of the CSL spin-label is that it distributes uniformly within the cholesterol-containing membranes, making it possible to probe the role of Chol on α-crystallin-membrane association.

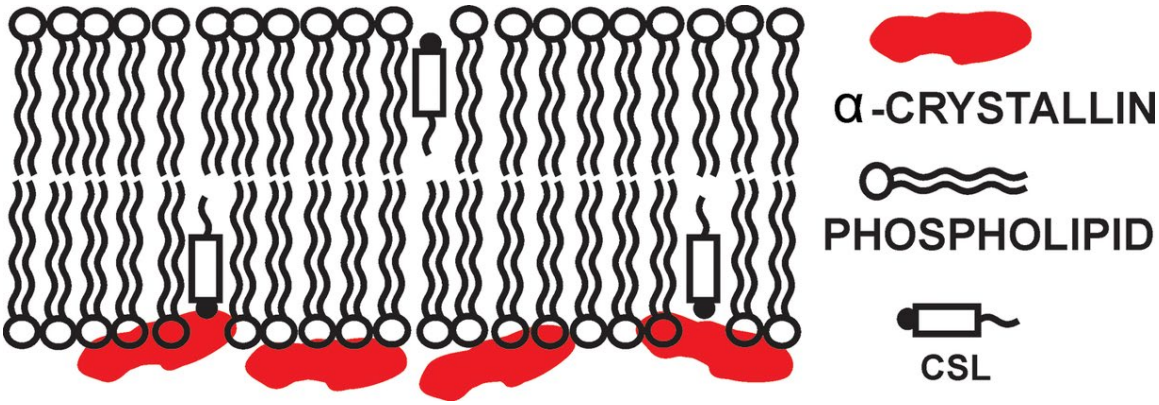

Figure 8 Schematic drawing showing the α-crystallin-membrane association and the approximate CSL spin-label location in the membrane.102

The PLs (DMPC, SOPC, DOPC, and PAPC), Chol, and CSL in chloroform solutions are mixed in a glass tube with 1 mol% of CSL spin-label maintained in PLs plus Chol solutions. The membrane samples were prepared with Chol/PL mixing ratios of 0 and 0.3. First, chloroform solutions were dried with a flow of N_2-gas to a volume of ~75 μL; then, we added 360 μL of HEPES buffer to the chloroform solution.

Then we continue preparing the Large Multilamellar Vesicles (LMVs) using the Rapid Solvent Exchange Method (RSE).[104,107,108] Figure 9 shows the RSE instruments in our laboratory. In the RSE instrument, the glass tube containing the HEPES buffer and chloroform mixture was connected to the sample manifold and placed on the vortexer. Then the vortexer was turned on, and the manifold connected to a vacuum system was opened, maintaining ~25 torr vacuum pressure. After 2 min, the controlled flow of argon

gas was passed through the manifold for ~10 s. The vacuum system evaporates the chloroform, and the argon flow further helps to evaporate the remaining traces of chloroform in the sample. Then, the sample tube was withdrawn from the RSE instrument. In this RSE process, chloroform is evaporated, and the lipids and CSL in the chloroform were rapidly transferred to the HEPES buffer, making LMVs with uniform distribution of CSL within the LMVs. The advantage of using RSE is that it maintains compositional homogeneity throughout the membrane suspension.[109,110]

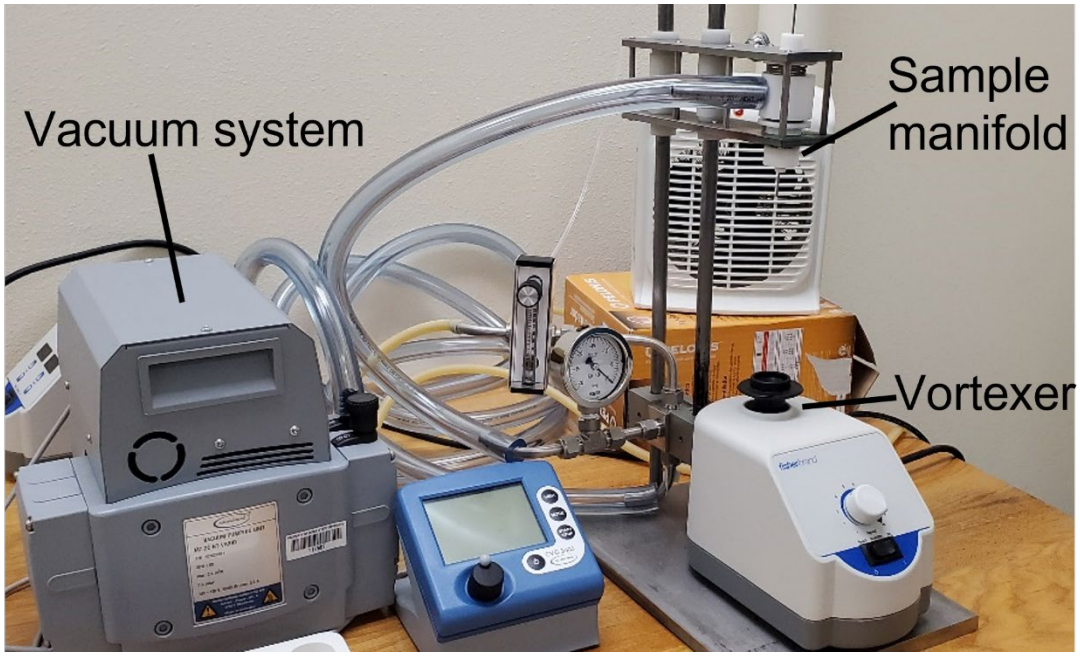

Figure 9 Custom Set Up of the Rapid Solvent Exchange Method.

A Probe-tip sonicator (Fisher Scientific, Model 550) was used to prepare Small Unilamellar Vesicles (SUVs) by sonicating LMVs ten to fifteen times with 10 s sonication and 15 s in ice for each sonication cycle.[103,104] The probe-tip sonicator was used at an energy level of ~ 30-45 Joules. Probe-tip sonication makes the sample hot; therefore, with each 10 s sonication, the sample tube was placed in ice for 15 s. Figure 10 shows the probe-tip sonicator in our laboratory. The conversion of milky suspensions of

LMVs into the transparent solutions of SUVs confirms the formation of SUVs after the probe-tip sonication process, shown in Figure 11.

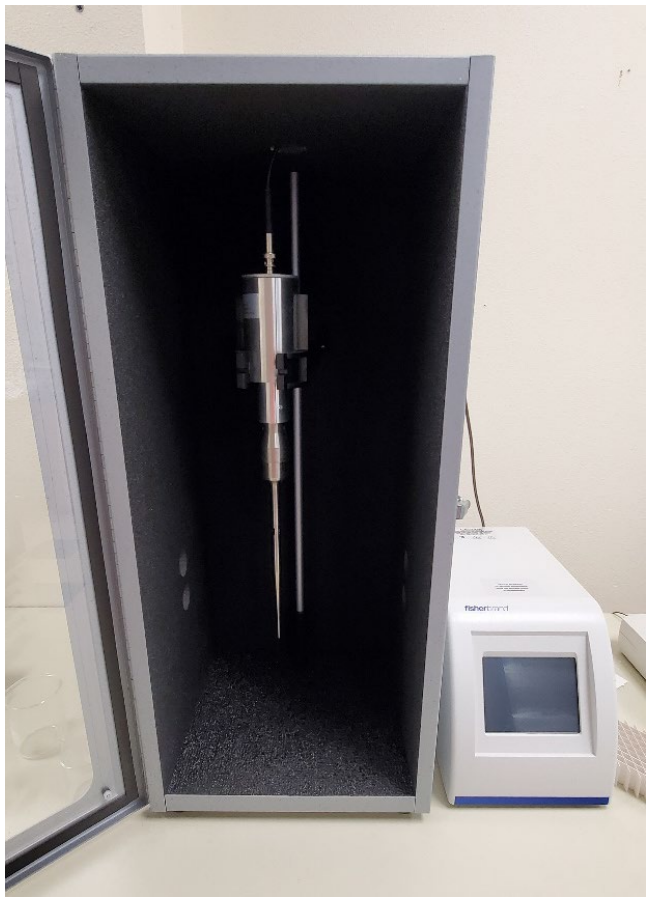

Figure 10 Probe-tip Sonicator.

The PLs plus Chol concentration in the SUVs samples was maintained at 40 mM. Since the autooxidation of the PL membrane depends on the number of double bonds on the acyl chain[111], we prepared the DOPC membrane containing one double bond on each acyl chain and PAPC membranes containing four double bonds on one acyl chain in an N_2-gas (oxygen-free) environment. It has been reported that the autooxidation of polyunsaturated PAPC membrane is very low for the first 75 h.[111]

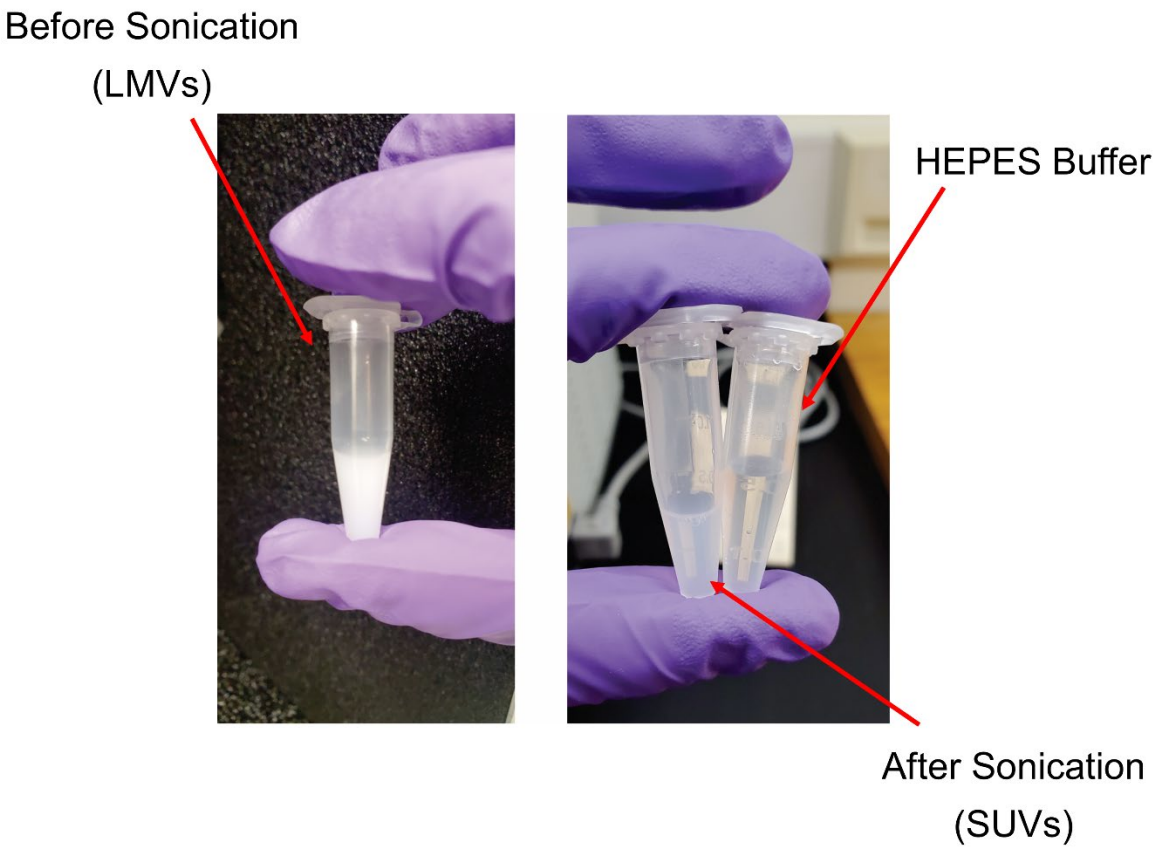

Figure 11 Before sonication, LMVs milky suspension (left). After sonication, SUVs semi-transparent suspension (right) with HEPES buffer as a reference to determine transparency.

The α-crystallin-membrane association is investigated by incubating α-crystallin with SUVs at 37 ºC for 16 h in a shaking incubator (Corning Inc., Corning, NY, USA). The shaking incubator in our laboratory is shown in Figure 12. The concentration of PLs plus Chol was fixed at 11.4 mM, and the concentration of α-crystallin was varied from 0 to 52.6 µM to monitor the α-crystallin-membrane association. To mimic the physiological temperature, we incubated α-crystallin and membrane samples at 37 ºC. The samples were incubated for 16 h because the association of α-crystallin with membranes is time-dependent, which saturates at ~8 h.[102]

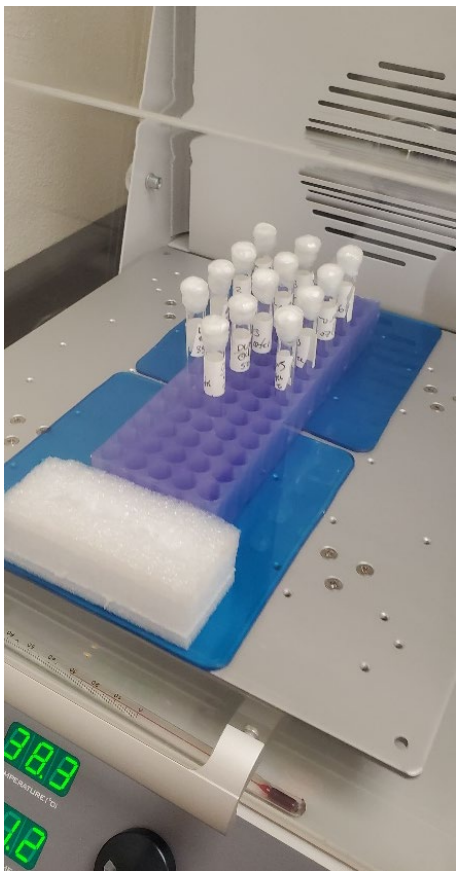

Figure 12 Membrane Samples Incubation Period at 37 ºC for 16 h in a shaking incubator in our laboratory.

Electron Paramagnetic Resonance (EPR) Experiments

The α-crystallin membrane samples incubated at 37 ºC for 16 h were filled into 0.8 mm internal diameter (i.d.) gas-permeable methylpentene polymer (TPX) capillary for EPR measurements at 37 ºC.[105] Figure 13 shows the TPX with 0.8 mm and 1 mm i.d. used in our laboratory. The free oxygen in the sample is paramagnetic and induced line-broadening of EPR spectra. Since the TPX capillaries used in our laboratory are gas permeable, the N_2-gas connected to our instrument passes through it and removes the free oxygen from the sample. So, we record the EPR signal at an oxygen-free environment. EPR experiments at – 165 ºC were performed using a 1.0 mm i.d. TPX capillary[105] to get a better signal-to-noise ratio at lower temperatures.

Figure 13 Gas-permeable methylpentene polymer (TPX) capillary used for EPR measurements; 0.8 mm (left) and 1.0 mm (right).

An X-band Bruker ELEXSYS 500 continuous-wave (CW) EPR spectrometer equipped with temperature-controlled accessories was used for the EPR measurements. The N_2-gas flow was used to deoxygenate the samples and maintain the temperature at 37 ºC, whereas, for low-temperature measurement, liquid nitrogen was used to maintain the temperature at – 165 ºC. For 37 ºC EPR measurement, CW EPR spectra were accumulated with microwave power and modulation amplitude of 8.0 mW and 1.0 G, respectively. For – 165 ºC measurement, microwave power of 2.0 mW and modulation amplitude of 2.0 G were used. As described in detail in our recent papers[102–104], a change in the EPR signal of the CSL spin-label, located near the headgroup regions of membranes, provides the unique opportunity to investigate the α-crystallin-membrane association. We found no significant change in the EPR signals of CSL in membranes

with incubation at 37 ºC for 16 h and without incubation (0 h incubation), indicating the stability of membranes.

EPR Instrument

The X-band Brucker ELEXSYS 500 CW-EPR in our laboratory is shown in Figure 14. It consists of a magnet that produces a magnetic field, a microwave bridge that produces a constant microwave with a frequency of 9.45 GHz, a resonator where the sample tube is located with a microwave field and the EPR resonance occurs, a power amplifier, and a control and signal processing unit. N_2-gas is continuously passed into the resonator from the back of the instrument, which maintains the temperature at 37 ºC and removes free oxygen from the sample. Liquid nitrogen is passed into the resonator from the back of the instrument to maintain the temperature at about -165 ºC.

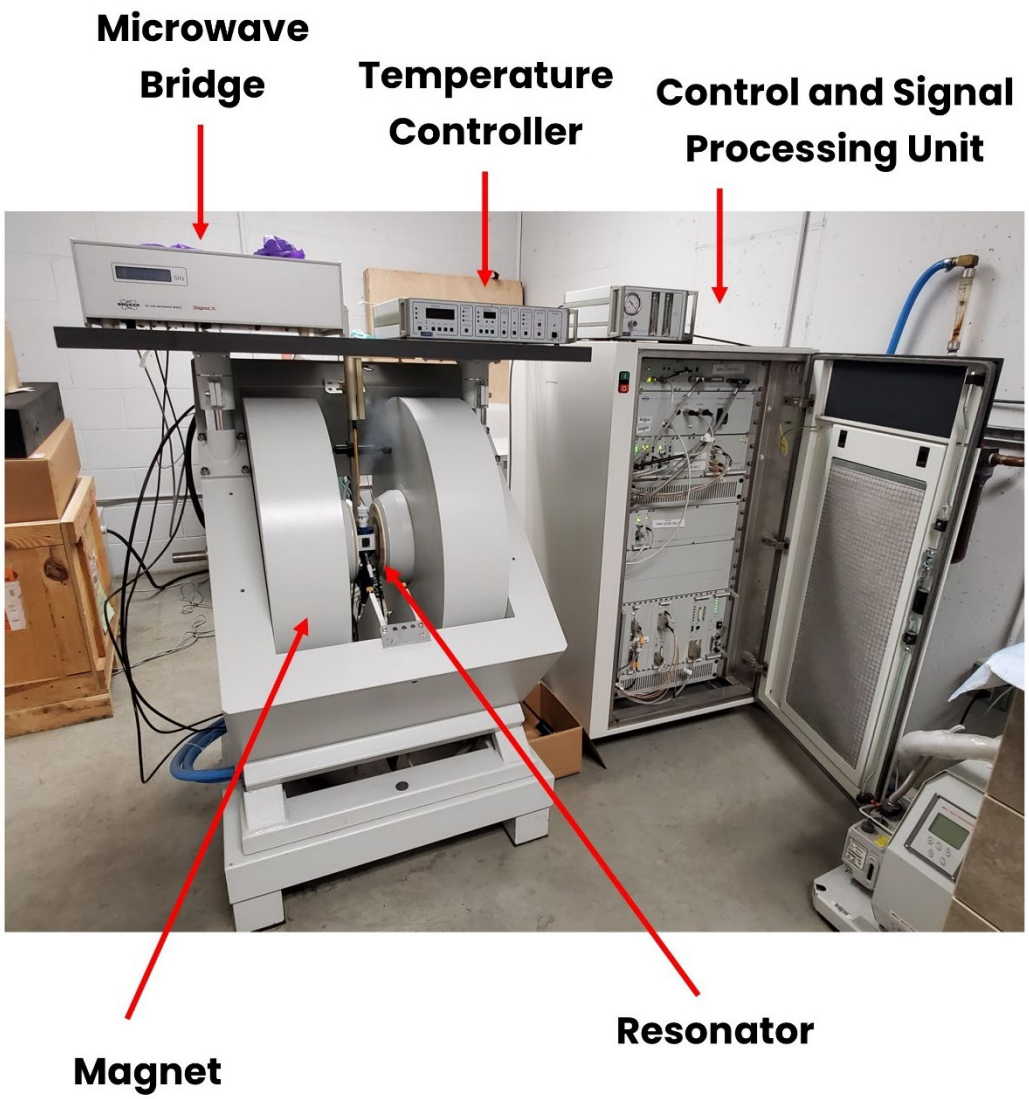

Figure 14 X-band Bruker ELEXSYS 500 continuous-wave (CW) EPR spectrometer in our laboratory.

A schematic of the components of the CW-EPR is shown in Figure 15. To enable phase-sensitive detection, the microwaves produced by the source are split into the microwave bridge's signal and reference arms. A frequency counter is often given small power to track the microwave frequency. The bias attenuator controls the microwave power in the reference arm, while the phase shifter regulates the relative phase between the signal and reference arms. The resonator receives the microwave through the

reference arm connected to the circulator, and an attenuator regulates the power reaching the sample in the resonator. The circulator confirms that only the reflected power from the resonator reaches the mixer. The resonator is connected to the microwave bridge by the iris, which controls the power in the resonator. Sweeping the magnetic field over a range of interest, an EPR transition enters resonance, and the sample absorbs microwaves. The first derivative of the absorption signal is the EPR spectrum.

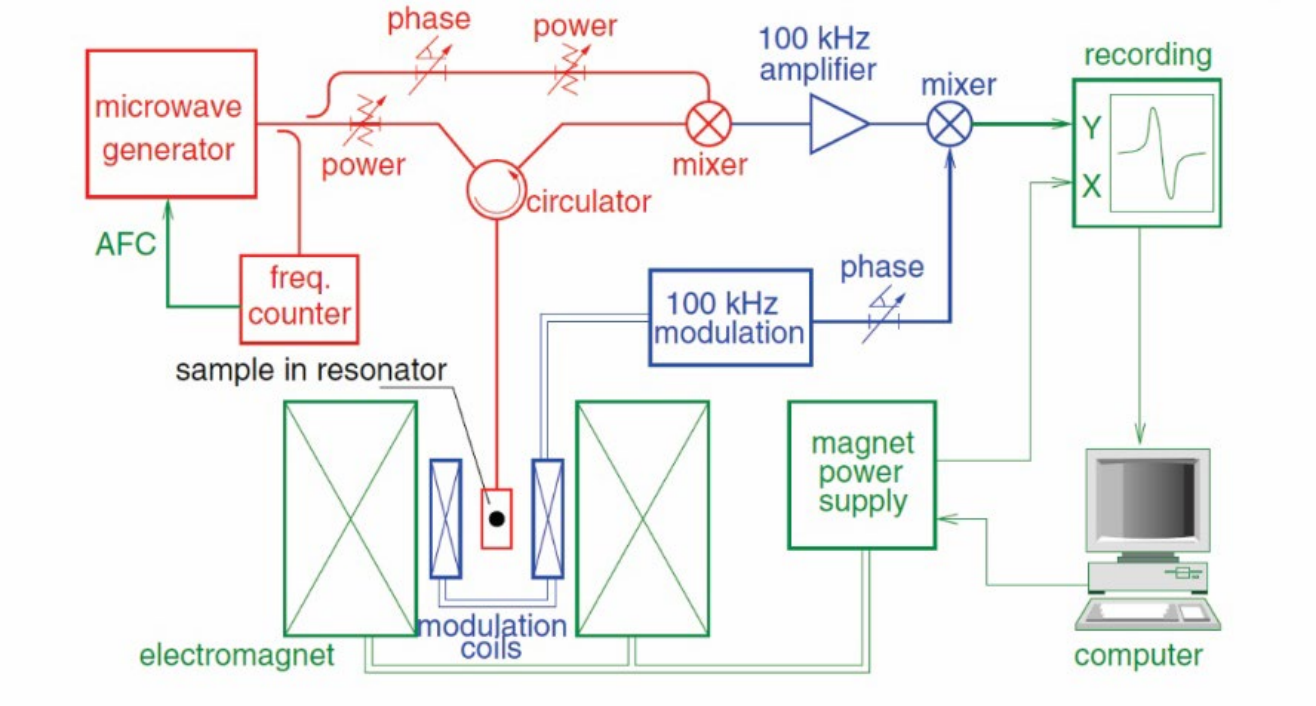

Figure 15 Schematic of the components of the CW EPR.112

EPR Theory

In an EPR experiment, a sample with the free electron is exposed to a microwave at a fixed frequency, and the magnetic field is varied until it matches the energy of the microwave, as represented by the double arrow in Figure 16. At this point, the unpaired electrons with spin quantum number S = 1/2 align parallel to the magnetic field with magnetic spin quantum number M_s = +1/2 or antiparallel to the magnetic field with a

magnetic spin quantum number M_s = -1/2. Due to the Zeeman effect, each alignment has energy given by:

$$E = M_s g_e \beta_e B_0 \quad (1)$$

B_0 is the magnetic field, g_e = 2.0023 is the free electron's g-factor, and β_e is the electron Bohr magneton.[113] The separation between two energy states is given by:

$$\Delta E = g_e \beta_e B_0 \quad (2)$$

An unpaired electron can move between the energy levels by absorption of the energy of the microwave radiation, i.e., hv, such that the resonance condition is obeyed given by the following equation:

$$\Delta E = hv = g_e \beta_e B_0 \quad (3)$$

The h is Planck's constant and v is the frequency of the microwave radiation. Our EPR experiments are conducted at 9.45 GHz, known as the "X-band frequency".[113] According to Boltzmann distribution, the number of spins in upper energy states is less than in the lower energy states in thermodynamic equilibrium. So, there is a net energy absorption, as shown by the dotted absorption spectra in Figure 16. The modulation amplitude applied in the EPR instrument takes the first derivative of the absorption spectra and produces the EPR spectra as shown in the spectra shown together with the dotted absorption spectra in Figure 16.

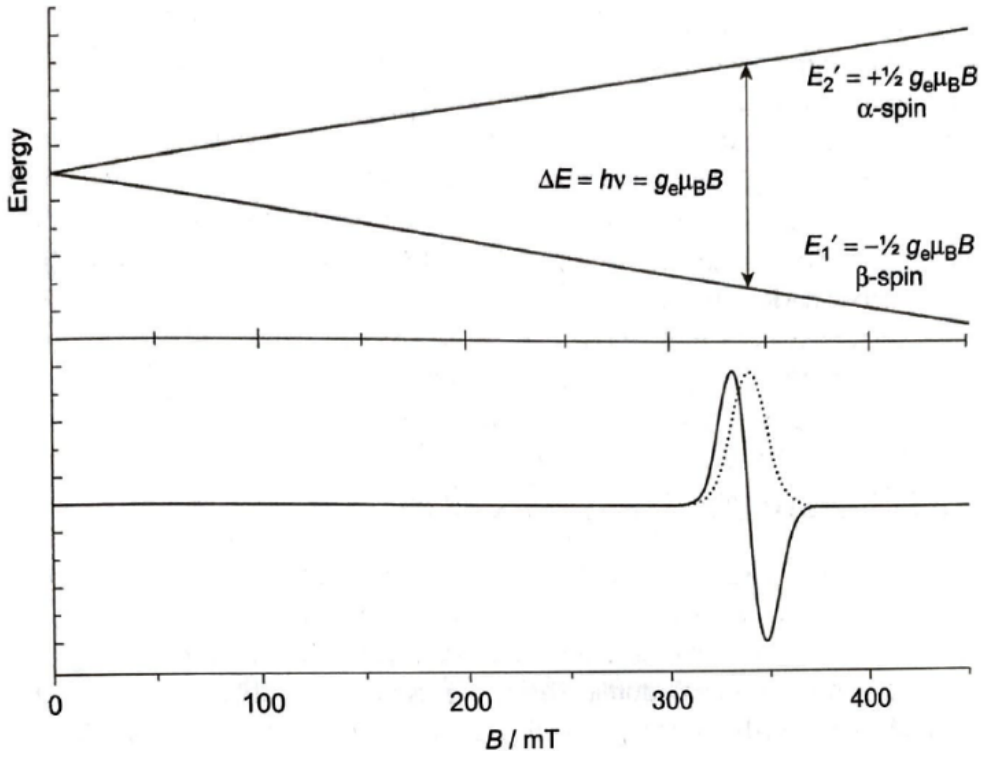

Figure 16 Zeeman Effect. Splitting of the electron's energy in the presence of a magnetic field.114 The bottom dotted spectrum is the absorption spectrum, and the spectrum, together with the absorption spectrum, is the EPR spectrum.

The nitroxide moiety of the spin-label (CSL spin-label in our case) has a ^{14}N isotope with the nuclear spin quantum number I = 1. Due to the hyperfine splitting, each electron spin ($M_s = \pm 1/2$) splits into three energy levels $M_I = -1, 0, +1$, giving rise to three possible transitions permitted by the selection rule $\Delta M_I = \pm 0$, as shown by the red arrows in Figure 17B. Corresponding to three possible transitions, three peaks are observed in the EPR spectra denoted by $M_I = +1$, 0, and -1, as shown in Figure 17C. Depending on the location of the nitroxide moiety in the lipid bilayer, the dynamics of the membrane along x-, y-, and z-directions differ, giving rise to different intensities of each peak in the EPR spectra.

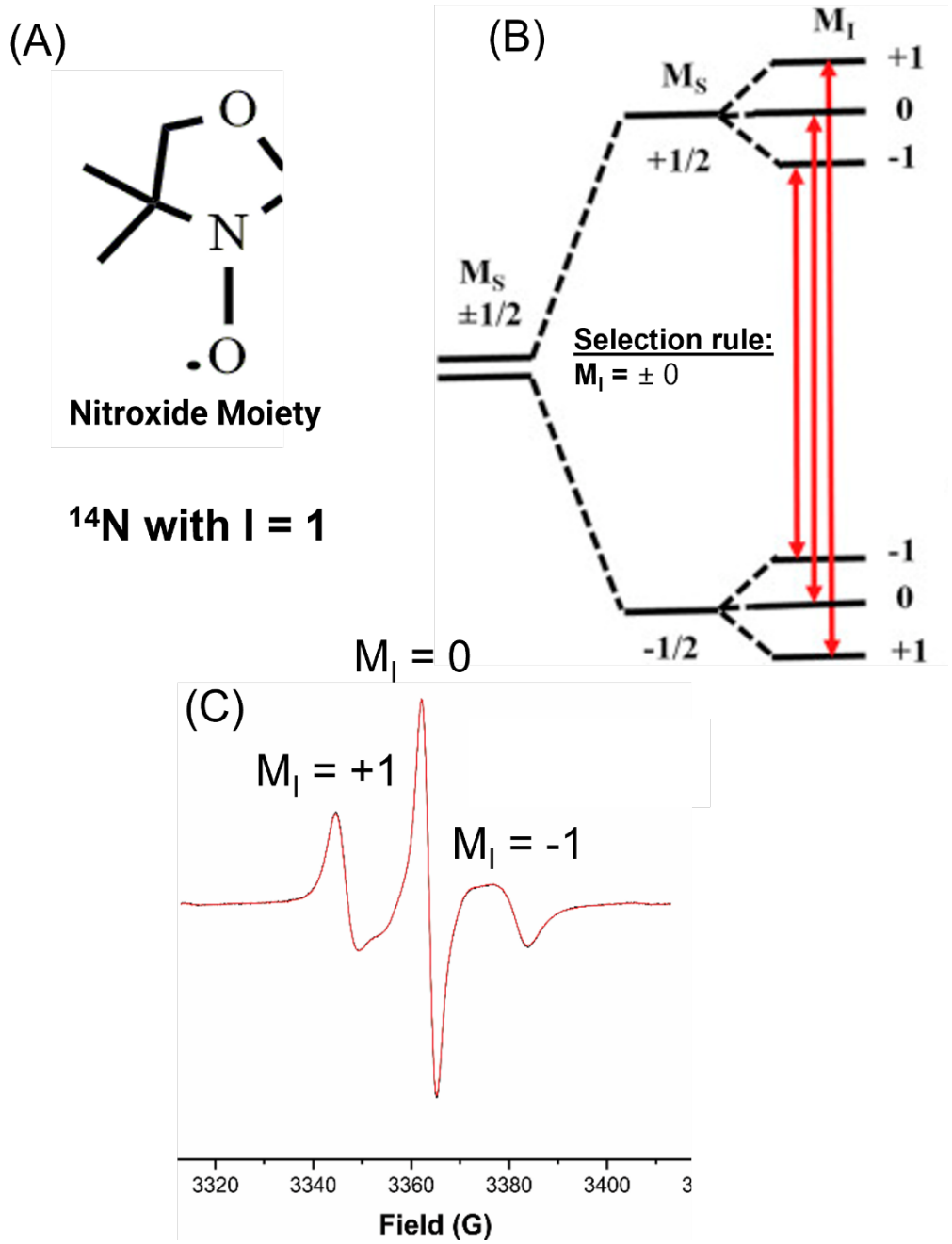

Figure 17 **Splitting of the electron's energy in the presence of the nitroxide moiety with a 14N isotope of the CSL spin-label. (A) Nitroxide moiety of the spin-label with 14N isotope with the nuclear spin quantum number I = 1. (B) Hyperfine splitting with the three possible transitions shown in red arrows, which are allowed by the selection rule MI = ± 0. (C) Three peaks in the EPR spectra correspond to the three possible transitions, as shown in (B).**

Measurements of the Percentage of Membrane Surface Occupied (MSO) and Association Constant (K_a)

After the EPR measurement, each spectrum was normalized with respect to peak-to-peak intensity of the central EPR line. The EPR approach to estimate the percentage of membrane surface occupied (MSO) by α-crystallin and the association constant (K_a) is based on the decrease in the peak-to-peak EPR signal intensity of the low field EPR line with α-crystallin association with membranes.[102–104] The representative normalized EPR spectra of CSL in the DOPC membrane in the absence of α crystallin (black) and 52.6 μM α-crystallin (red) are shown in Figure 18A. Figure 18B shows the zoomed low field lines of the spectra shown in Figure 18A. The peak-to-peak intensity of the low field EPR decreases due to the association of α-crystallin to the DOPC membrane, as shown by the decreased peak-to-peak intensity of the low field line of the EPR spectra in the presence of 52.6 μM α-crystallin as shown in Figure 18B. In previous works[102–104], we observed a similar decrease in the peak-to-peak EPR signal intensity of the low field EPR line with α-crystallin association with membranes. Figure 18C shows the representative normalized EPR spectra of CSL in Chol/DOPC membrane with Chol/DOPC mixing ratio of 0.3 in the absence of α crystallin (black) and with the presence of 52 6 μM α-crystallin (red). Figure 18D shows the zoomed low field EPR lines of the spectra shown in Figure 18C. No change in the peak-to-peak intensity of the low field EPR lines of the spectra for the Chol/DOPC membrane with Chol/DOPC mixing ratio of 0.3 in the presence of 52.6 μM α-crystallin represents that there is no association of α-crystallin with this membrane.

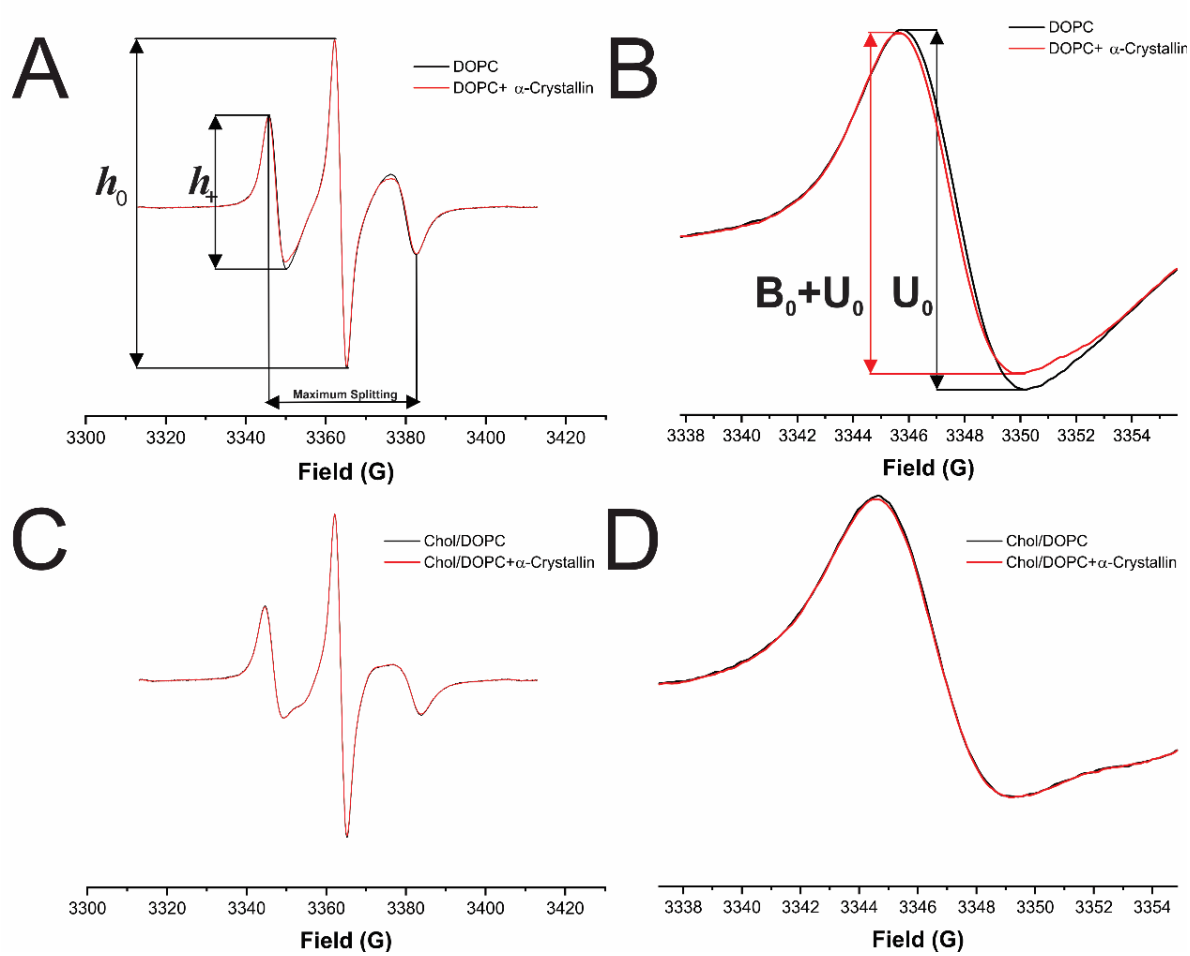

Figure 18 A) EPR spectra of CSL in DOPC membrane in the absence of α crystallin (black) and 52 6 µM α-crystallin (red). Ratio of peak-to-peak intensity of low field line (h+) and the central line (h0) is used to calculate the mobility parameter (h+/h0). The horizontal distance between the low field and high field lines in the EPR spectra is used to calculate the maximum splitting. B) Zoomed low field line of the EPR spectra shown in Figure 17A. The peak-to-peak intensities of low field EPR line of unbound (U0) and unbound plus bound (U0+B0) contributions are used to calculate the percentage of membrane surface occupied (MSO) and binding affinity (Ka). C) EPR spectra of CSL in Chol/DOPC membrane with the Chol/DOPC mixing ratio of 0.3 in the absence of α crystallin (black) and 52 6 µM α-crystallin (red). D) Zoomed low field line of the EPR spectra shown in Figure 17C.

To calculate the MSO and K_a, the EPR spectra without α-crystallin were used as unbound (U_0), and the EPR spectra with α-crystallin was used as unbound plus bound ($U_0 + B_0$) contributions, as shown in Figure 18B. As previously shown in Figure 8, α-crystallin associates on the outer surface of the membrane, and the CSL spin-label is

located near the head group region of the membrane. To calculate the percentage of CSL spin-label affected by the association of α-crystallin, we used the following equation.[102–104]

$$\%\ CSL\ spin\ labels\ affected = \{U_0 - (B_0 + U_0)\}(U_0)^{-1}100\% \quad (4)$$

The diameter of the SUVs is estimated to be ~30 nm, as in our previous studies.[102–104] Therefore, ~60% of the CSL spin-labels are near the outer surface, and ~40% of the CSL spin-labels are near the inner surface of the membrane.[104] The α-crystallin associates on the outer membrane surface and affects the CSL spin-labels that are on the outer surface of the membrane. Therefore, the corrected % of the CSL spin label affected by the α-crystallin association or the MSO by α-crystallin is acquired by multiplying equation (3) by the correction factor (100/60):

$$\%\ MSO = (\%\ CSL\ spin\ label\ affected)(100/60) \quad (5)$$

MSO offers quantitative data regarding the percentage of outer surface occupied by α-crystallin. MSO is plotted as a function of α-crystallin concentration, and the data points are fitted with a one-site ligand binding model using GraphPad Prism (San Diego, CA) [102–104]: The equation of the one-site ligand binding model is as follows:

$$Y = (XB_{max})(K_d + X)^{-1} \quad (6)$$

Where B_{max} represents the maximum specific association and provides the extrapolation of the MSO by a very high concentration of α-crystallin, and K_d is the dissociation constant, providing the α-crystallin concentration needed to achieve a half-maximum association at equilibrium. B_{max} and K_d have the same units as Y and X,

respectively.[102–104] Since the membrane's outer surface regions are identical, the α-crystallin can associate with any region of the membrane's outer surface with equal probability. Therefore, a one-site ligand binding model was used to determine the K_d. The association constant (K_a) is calculated as follows [102–104]:

$$K_a = {K_d}^{-1} \tag{7}$$

K_a provides information on how fast the maximum percentage of membrane surface occupied (MMSO) is achieved. In other words, the K_a provides information about the strength of the α-crystallin association with the membranes. The higher the value of K_a, the stronger the α-crystallin association with the membrane and vice-versa.

Measurement of Physical Properties of the Membrane

The physical properties of the membranes measured are the maximum splitting, mobility parameter, and hydrophobicity near the surface of membranes. The mobility parameter and maximum splitting are obtained from the EPR signal recorded at 37 ºC, and hydrophobicity ($2A_z$) is obtained from the EPR signal recorded at about –165 ºC. The mobility parameter gives information about the mobility (dynamics) change near the headgroup region of membranes with α-crystallin association.[102–105] The maximum splitting provides information about the order near the headgroup region of membranes with α-crystallin association.[102–105] As mentioned, CSL is present in the outer and inner surfaces of the membrane. The mobility parameter and maximum splitting provide the average effect of the CSL spin labels from both surfaces of the membrane. The ratio of the peak-to-peak intensity of the low field and central field EPR line (i.e., h_0/h_+) provides the mobility parameter, and the horizontal distance between the low and high field lines in EPR spectra provides the maximum splitting, as shown in Figure 18A. Figure 19

shows the representative EPR spectra of CSL in the SOPC membrane at about -165 ºC. The hydrophobicity measured with the CSL spin-label provides information about the surface hydrophobicity near the headgroup regions of membrane.[105] As shown in Figure 19, the horizontal distance between the low and high field ERP lines of the spectra taken at about -165 ºC gives $2A_z$, where a decrease in the $2A_z$ value means an increase in hydrophobicity (decrease in polarity).[115–119]

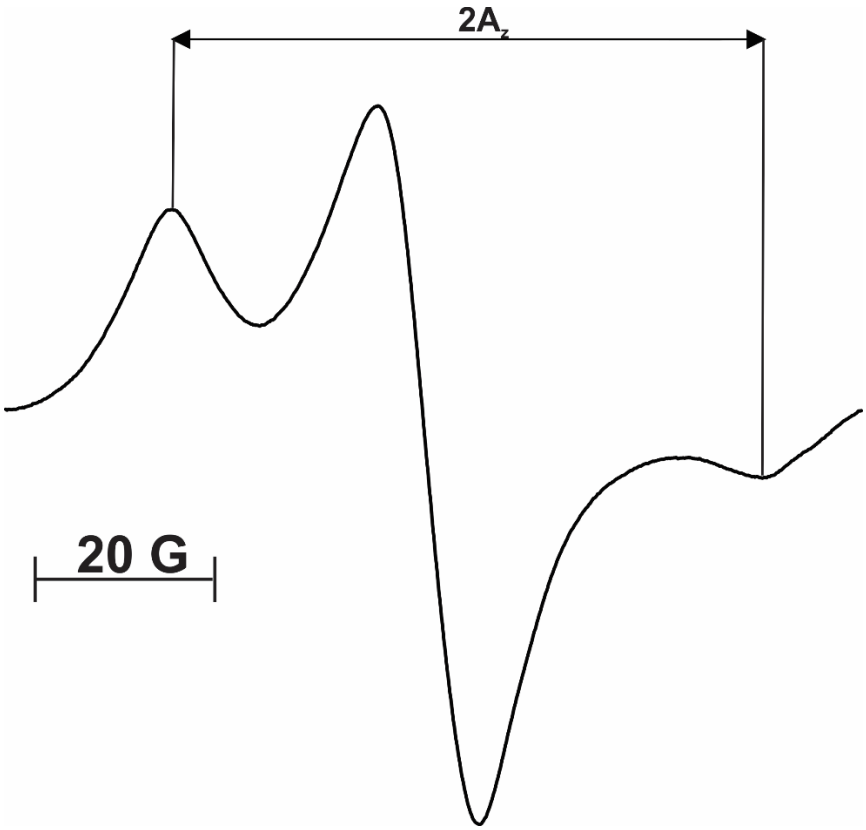

Figure 19 EPR spectra of CSL in SOPC membrane at about -165 ºC

Statistics

The statistically significant difference in the maximum percentage of membrane surface occupied (MMSO), K_a, mobility parameter, maximum splitting, and hydrophobicity is determined using a Student's t-test with $p \leq 0.05$ as the statistical significance criterion. The MMSO value is the MSO value obtained after achieving

saturable binding. All the data are obtained from three independent experiments and expressed with mean ± standard deviation.

CHAPTER 4: RESULTS AND DISCUSSION

MSO by α-Crystallin on Saturated, Monounsaturated, and Polyunsaturated Membranes

For all Chol-free membranes (Chol/PC mixing ratio of 0), MSO by α-crystallin increases with an increase in α-crystallin concentration, as shown in Figure 20, representing the increase in the α-crystallin-membrane association. However, the MSO increases rapidly with the rapid saturable association of α-crystallin with DMPC and SOPC membranes compared to DOPC and PAPC membranes. Saturable association of α-crystallin with a lipid membrane was reported previously.[92,120,121] We recently observed the saturable association of α-crystallin with membranes made of individual, two-component, and four component lipid mixtures.[18,102–105] All the membranes investigated in this study have the same headgroup but different chain lengths and degrees of acyl chain unsaturation. The different rates to achieve the saturable association of α-crystallin (i.e., MSO by α-crystallin per increase in α-crystallin concentration) with different membranes (Figure 20) suggest that the acyl chain length and degree of unsaturation determine how quickly the saturable association is observed with membranes. As shown in Figure 7, the DMPC membrane has both acyl chains saturated (no double bonds) with 14 carbon atoms in each acyl chain (i.e., 14:0–14:0 PC), the SOPC membrane has one acyl chain saturated and another acyl chain monounsaturated with 18 carbon atoms in each acyl chain (i.e., 18:0–18:1 PC), the DOPC membrane has both acyl chains monounsaturated with 18 carbon atoms in each acyl chain (i.e., 18:1–18:1 PC), and

PAPC membrane has one acyl chain saturated with 16 carbon atoms and another acyl chain polyunsaturated with four double bonds with 20 carbon atoms (i.e., 16:0–20:4 PC). Figure 20 shows that the rate to achieve the saturable association of α-crystallin follows the trends: DMPC > SOPC > DOPC ≈ PAPC, suggesting that the membrane with a shorter acyl chain length and a higher degree of saturated chain achieves the binding saturation at a faster rate. The MMSO by α-crystallin follows the trends: SOPC ≈ DOPC > DMPC ≈PAPC. The MMSO by α-crystallin with DMPC and SOPC membranes are ~6.1% and ~8.3%, respectively, and the difference in these MMSO values is statistically significant with $p \leq 0.05$. The MMSO by α-crystallin with DOPC and PAPC membranes are ~8% and ~5.9%, respectively, and the difference in these MMSO values is statistically significant with $p \leq 0.05$. The combined results for DMPC, SOPC, DOPC, and PAPC suggest that how quickly the binding saturation is achieved and the MMSO by α-crystallin is determined by the synergistic effect of both acyl chain length and degree of unsaturation of acyl chains. The MMSO values for Chol-free membranes (Figure 20) are comparable to the MMSO values obtained from previous research, i.e., ~2% to ~13%, with membranes made of individual lipid, two-component lipid mixtures, and four-component lipid mixtures using an EPR spin-label approach.[102–105] The MMSO values for Chol-free membranes (Figure 20) are also comparable to the results obtained by Mulders et al.[122], where they labeled α-crystallin with [35S] methionine and incubated with PC vesicles and found that approximately 10% of α-crystallin associated with PC vesicles. We previously investigated the association of α-crystallin with membranes made of individual lipids (i.e., POPC, POPS, and POPE) and two-component lipid mixtures (i.e., SM/POPC, SM/POPS, and SM/POPE), having the same acyl chain length and degree of

unsaturation but different lipid headgroups, and found that MMSO by α-crystallin and the rate to achieve the binding saturation is modulated by lipid headgroup's charge and size, lipid curvature, and hydrogen bonding between lipid headgroups.[103] In this research, we kept the lipid headgroup fixed and varied acyl length and degree of unsaturation (see Figure 7 for lipid structure) and found that acyl chain length and degree of unsaturation strongly modulate α-crystallin membrane association (Figure 20). Previously, Tang et al.[91] reported that the association of α-crystallin with lipid membrane depends on acyl chain order. However, Cobb and Petrash[84] reported that acyl chain length, unsaturation, and lipid headgroup and type do not influence α-crystallin-membrane association. The earlier infrared spectroscopy study suggests that the lipid headgroup mediates α-crystallin-membrane interactions.[123]

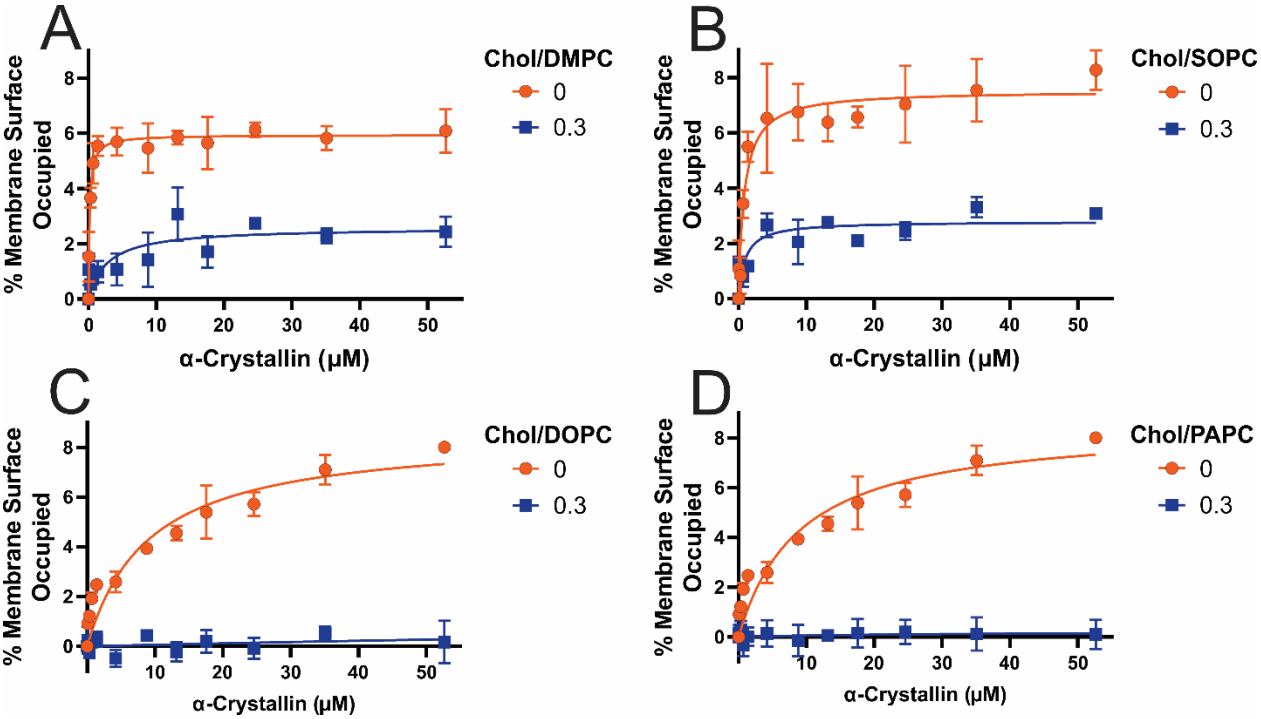

Figure 20 (A–D) Percentage of membrane surface occupied (MSO) plotted as a function of α-crystallin concentration for A) Chol/DMPC, B) Chol/SOPC, C) Chol/DOPC, and D) Chol/PAPC membranes, respectively, at Chol and PL mixing ratios of 0 and 0.3. The rate of increase of MSO with respect to α-crystallin concentration is different for different PC membranes, showing that acyl chain length and degree of unsaturation of PC membranes modulate the α-crystallin-membrane association. Independent of the PC lipid type, Chol decreases the MSO, representing that Chol inhibits the α-crystallin-membrane association. The data points are expressed as mean ± standard deviation from three independent experiments and fitted using a one-site ligand binding model in GraphPad Prism (San Diego, CA, USA) to calculate the association constant (Ka).

With a Chol/PC mixing ratio of 0.3 (Figure 20), the MSO by α-crystallin sharply decreases close to zero for polyunsaturated membranes (i.e., Chol/DOPC and Chol/PAPC); however, it decreases ~60% for saturated (i.e., DMPC) and monounsaturated (i.e., SOPC) membranes. MMSO values, when compared with and without Chol, show a statistically significant difference with $p \leq 0.05$ for all PC membranes. These results suggest that Chol decreases the MSO by α-crystallin; however, the decrease level depends on the acyl chain length and degree of unsaturation. We have recently found a similar decrease in MSO by α-crystallin in the presence of Chol for

membranes with different headgroups but the same acyl chain length and degree of unsaturation; however, the level of decrease depends upon the lipid headgroup type.[104] Previously, Tang et al.[91] investigated the association of α-crystallin with Chol/distearoyl-phosphatidylcholine (DSPC), Chol/SM, and Chol/egg PC membranes using a fluorescence approach and found that Chol decreases the α-crystallin association with DSPC and SM membranes but increases the α-crystallin association with egg PC membrane. In contrast, Cobb and Petrash[84] used AlexaFluor350TM-conjugated α-crystallin and found no significant association of α-crystallin with and without Chol in PC and SM membranes. The surface hydrophobicity of DMPC, SOPC, DOPC, and PAPC membranes decreases with an addition of Chol, irrespective of the acyl chain length and degree of unsaturation. The decrease in surface hydrophobicity with the corresponding decrease in MSO with the addition of Chol suggests that the α-crystallin interacts with the membrane via hydrophobic interaction.

K_a of α-Crystallin Association with Saturated, Monounsaturated, and Polyunsaturated Membranes

The K_a gives the strength of α-crystallin-membrane association. The higher the K_a, the stronger the α-crystallin-membrane association. If α-crystallin does not associate with the membrane, the MSO and K_a values are both 0. The value of K_a is determined by how quickly the MSO increases if α-crystallin is associated with the membrane. In other words, K_a provides a quantitative estimate of how quickly the MMSO is occupied, and there may be different values of K_a for the same MMSO. The K_a follows the trends: K_a (Chol/DMPC) > K_a (Chol/SOPC) > K_a (Chol/DOPC) ≈ K_a (Chol/PAPC), both for membranes in the presence and absence of Chol, as shown in Figure 21. The K_a for the

DMPC membrane is about five times higher than the SOPC membrane and about 50 times higher than that of DOPC and PAPC membranes, suggesting that K_a is significantly higher for saturated membranes with a shorter acyl chain length. Even the MMSO is similar between DMPC and PAPC, SOPC and DOPC, and Chol/DMPC and Chol/SOPC membranes, the significantly different values of K_a for these membranes are attributed to these lipids' significantly different acyl chain lengths and degrees of unsaturation. Previously, we estimated the K_a for POPC (i.e., 16:0–18:1 PC) membrane to be 4.9 ± 2.4 μM^{-1}.[102] In the present study, K_a for the SOPC (i.e., 18:0–18:1 PC) membrane is 1.15 ± 0.2 μM^{-1}, which is about four times smaller than the K_a for the POPC membrane. The only difference between the SOPC and POPC membranes is that one of the acyl chains in the POPC membrane is two carbon atoms shorter than the SOPC membrane. This clearly shows that the shorter the acyl chain length, the higher is the K_a of α-crystallin membrane association. The K_a for SOPC and DOPC membranes are 1.15 ± 0.22 μM^{-1} and 0.11 ± 0.02 μM^{-1}, respectively. The SOPC and DOPC membranes have 18 carbon atoms in their acyl chains. However, the SOPC membrane has only one acyl chain monounsaturated (i.e., 18:0–18:1 PC), whereas the DOPC membrane has both the acyl chains monounsaturated (i.e., 18:1–18:1 PC). Approximately ten times larger K_a for the SOPC membrane than the DOPC membrane clearly shows that the increase in the number of double bonds in the acyl chains (i.e., increase in the level of unsaturation) significantly decreases the K_a, playing a critical role in the α-crystallin-membrane association. The K_a values for DOPC and PAPC membranes and Chol/DOPC and Chol/PAPC membranes are similar with no statistically significant difference with a p-value ≤ 0.05. Other than these membranes, the K_a values among different membranes and within the same

membrane with different Chol content have a statistically significant difference with a p-value ≤ 0.05. The PAPC membrane has one acyl chain saturated, and another acyl chain with 20 carbon atoms is polyunsaturated with four double bonds (i.e., 16:0–20:4 PC). The similar K_a values for the DOPC and PAPC membranes suggest the synergistic effects of unsaturation of acyl chain, level of polyunsaturation (number of double bonds on acyl chain), and length of acyl chains on α-crystallin-membrane association. Our previous K_a measurements for membranes having the same acyl chain length and degree of unsaturation, but different headgroups (i.e., POPC, POPS, POPE, SM/POPC, SM/POPS, and SM/POPE membranes) show K_a differs significantly for membranes due to the difference in their headgroups.[102,103] This suggests that the acyl chain length and degree of acyl chain unsaturation modulate α-crystallin-membrane association. Lipid composition in the human lens membrane changes significantly with age, increasing the saturation of the acyl chains (i.e., decreasing the double bonds) and decreasing the length of the lipid acyl chain.[80–84] The data presented in this study show that shorter acyl chain length and a higher degree of acyl chain saturation significantly increase the K_a of α-crystallin-membrane association. This may be one of the reasons why the association of α-crystallin with the lens membrane increases with age.[18,84,95,124–126] The estimated K_a values (Figure 21) are comparable to the K_a values obtained for the membranes made of individual lipid[102,103], two-component lipid mixtures[103], and four-component lipid mixtures.[105] Moreover, the K_a values reported in this study are comparable to the K_a value of 7.69 μM^{-1} reported earlier by Mulders et al.[122] for the α-crystallin association with alkali-washed lens plasma membranes.

Figure 21 shows that, independently of the acyl chain length and degree of unsaturation, Chol inhibits the association of α-crystallin with Chol/DMPC, Chol/SOPC, Chol/DOPC, and Chol/PAPC membranes; however, the level of inhibition is different for different membranes. In the Chol/DMPC membrane, K_a decreases by a factor of about six times when compared to K_a of the Chol-free DMPC membrane; however, in the case of the Chol/SOPC membrane, K_a decreases by a factor of about three times when compared to Chol-free SOPC membrane (Figure 21). The addition of Chol separates the headgroups of the membrane, increasing the water accessibility (decreasing hydrophobicity) near the headgroup regions, ultimately reducing the strength (K_a) of the likely hydrophobic α-crystallin-membrane association. The higher decrease in K_a values for Chol/DMPC membrane compared to Chol/SOPC membrane with the addition of Chol can be explained based on the corresponding decrease in the surface hydrophobicity of membranes. Our recent research investigating the association of α-crystallin with models of human, porcine, and mouse lens-lipid membranes shows that the surface hydrophobicity of membranes and K_a decrease with increased Chol content, suggesting the hydrophobic interaction of α-crystallin to the model lens-lipid membranes.[105] With the addition of Chol, the surface hydrophobicity of the DMPC membrane decreases significantly from its initial value compared to the SOPC membrane, which may be why the K_a for the Chol/DMPC membrane decreases significantly compared to the Chol/SOPC membrane. For Chol/DOPC and Chol/PAPC membranes, K_a decreases significantly close to 0 with the addition of Chol, like MSO (Figure 20), implying no significant association of α-crystallin with these membranes. Our results show that Chol inhibits α-crystallin membrane association; however, the synergistic effect of lipid acyl

chain length and degree of unsaturation of membranes strongly modulate the level of inhibition. Previously, we investigated POPC and POPS membranes with the same acyl chains and degree of unsaturation but with different headgroups.[102,103] 50 mol% Chol completely inhibits α-crystallin association with the POPC membrane, but 60 mol% Chol does not completely inhibit α-crystallin association with the POPS membrane, suggesting that the lipid headgroups modulate the level of inhibition of α-crystallin association with membranes.[102,103] The combined results of our previous studies[102,103] and the study reported in this paper suggest that the acyl chain length, degree of acyl chain unsaturation, and lipid headgroups modulate α-crystallin-membrane association.

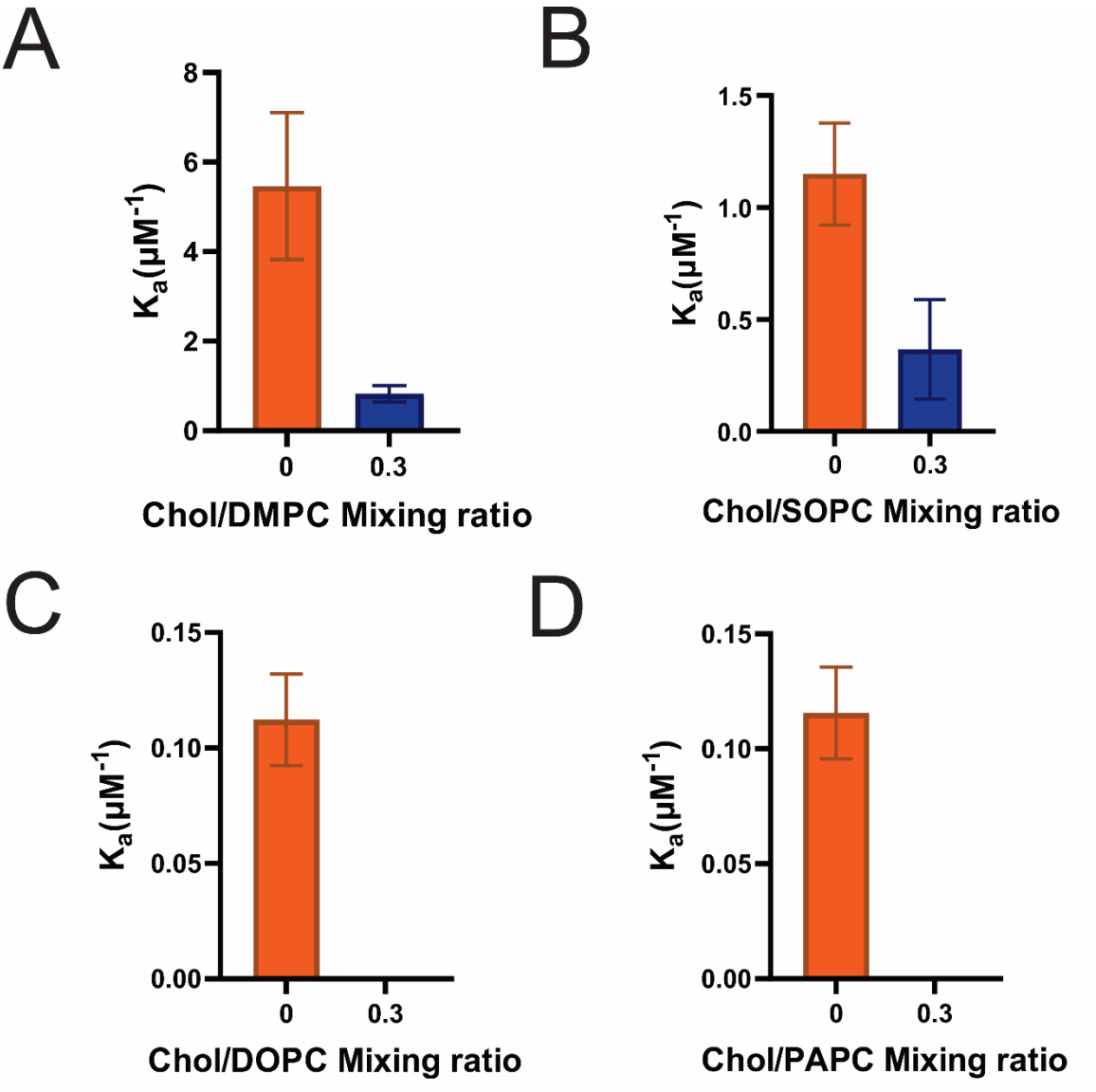

Figure 21 **(A–D) Association constant (Ka) of α-crystallin association with A) Chol/DMPC, B) Chol/SOPC, C) Chol/DOPC, and D) Chol/PAPC membranes, respectively, at Chol and PL mixing ratios of 0 and 0.3. The Ka was calculated by fitting the MSO versus α-crystallin concentration data shown in Figure 20 using a one-site ligand binding model in GraphPad Prism (San Diego, CA). The Ka is different for different PC membranes, representing that acyl chain length and degree of unsaturation strongly modulate the α-crystallin-membrane association. Moreover, the addition of Chol to the PC membranes decreases the Ka, representing that Chol inhibits the α-crystallin membrane association. The different levels of decrease in Ka for different membranes with the addition of Chol further show that acyl chain length and degree of unsaturation strongly modulate the α-crystallin-membrane association. The data points are expressed as mean ± standard deviation from three independent experiments.**

Mobility Parameter of Saturated, Monounsaturated, and Polyunsaturated Membranes with the α-Crystallin Association

The mobility parameter obtained from the CSL spin-label near the membrane surface gives information about the orientational and rotational dynamics near the headgroup regions of the membrane.[102–104,117,118,127] In the absence of Chol and α-crystallin, the mobility parameter of membranes follows the trends: DOPC > PAPC > SOPC > DMPC, as shown in Figure 22, indicating that dynamics near the headgroup regions of membranes decrease with the decrease in the degree of unsaturation of acyl chains (i.e., the decrease in the double bonds in acyl chain), with the degree of unsaturation of both acyl chains contributing to the mobility parameter. For Chol-free DMPC, SOPC, DOPC, and PAPC membranes, the mobility parameter values are statistically significant with a p-value ≤ 0.05. Interestingly, the trends of K_a of α-crystallin association with membranes (Figure 21) are the same as the reverse trends of the mobility parameter of membranes (Figure 22). The K_a is significantly high with significantly low mobility near the headgroup regions of saturated (DMPC) and monounsaturated (SOPC) membranes, suggesting that less mobile membranes have significantly higher K_a. The mobility parameter of the DOPC membrane is greater than the PAPC membrane, suggesting that one double bond in each acyl chain of the DOPC membrane effectively increases the mobility parameter than four double bonds in only one acyl chain of the PAPC membrane. For all Chol-free membranes (Figure 22), the mobility parameter decreases with an increase in α-crystallin concentration, indicating that the membrane regions near the headgroup become more immobilized with the α-crystallin-membrane association. It is clear from Figure 22 that the acyl chain length and

degree of unsaturation of membranes determine how fast the mobility parameter decrease with α-crystallin concentration. For the DMPC membrane (Figure 22A) with both acyl chains saturated and with shorter chain length, the mobility parameter decreases sharply with α-crystallin concentration, indicating that the membrane rapidly becomes more immobilized near the headgroup regions. However, for the SOPC membrane (Figure 22B) with longer acyl chains with one chain monounsaturated and other chain saturated, the mobility parameter decreases sharply but not as sharply as in the DMPC membrane. In polyunsaturated DOPC and PAPC membranes (Figure 22 C,D), the mobility parameter decreases slowly with an increase in α-crystallin concentration, indicating that the membranes slowly become more immobilized near the headgroup regions with an increase in α-crystallin concentration. All the membranes investigated here have the same lipid headgroup but varying acyl chain length and degree of unsaturation. The profiles of mobility parameter presented in Figure 22 clearly show that the acyl chain length and degree of unsaturation strongly modulate membrane dynamics near the head group regions with and without α-crystallin association. Previously, we investigated membranes with the same acyl chain length and degree of unsaturation but different headgroups and found that the lipid headgroup strongly modulates the mobility parameter near the headgroup regions of membranes with and without α-crystallin association.[102,103]

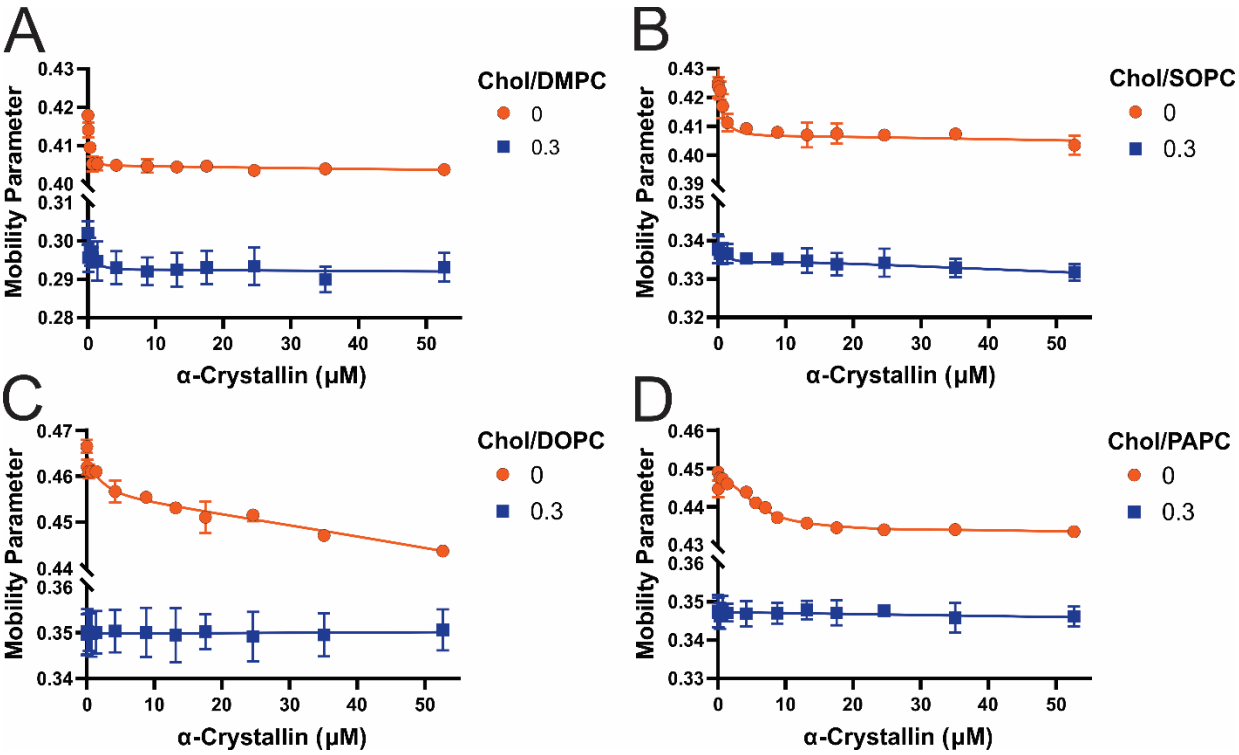

Figure 22 (A–D) Show the profiles of the mobility parameter (h+/h0) plotted as a function of α-crystallin concentration for A) Chol/DMPC, B) Chol/SOPC, C) Chol/DOPC, and D) Chol/PAPC membranes, respectively, at Chol and PL mixing ratios of 0 and 0.3. The mobility parameters are different for different PC membranes, showing that the mobility near the headgroup regions of membranes depends on the acyl chain length and degree of unsaturation of membranes. For all Chol-free membranes, the mobility parameter decreases with an increase in α-crystallin concentration, representing that these membranes become more immobilized near the headgroup region with the α-crystallin association. The addition of Chol decreases the mobility parameter of membranes, representing that these membranes regions near the headgroup become more immobilized with increased Chol content. However, the decrease in mobility parameter with increased α-crystallin concentration is less pronounced with the addition of Chol in the membranes, showing that Chol inhibits α-crystallin-membrane association. With increased α-crystallin concentration, mobility parameters of Chol/DMPC and Chol/DOPC membranes decrease, unlike for the Chol/DOPC and Chol/PAPC membranes, further showing that the acyl chain length and degree of unsaturation strongly modulate the mobility near the headgroup regions of membranes. The data points are expressed as mean ± standard deviation from three independent experiments, and the solid lines serve as the visual guides.

With the addition of the Chol, independently of the acyl chain length and degree of unsaturation, the mobility parameter decreases significantly for all membranes (Figure 22), indicating that the regions of the membranes near the headgroup become more

immobilized in the presence of Chol. In the presence of Chol and absence of α-crystallin, the mobility parameter follows the trends: Chol/DOPC ≈ Chol/PAPC > Chol/SOPC > Chol/DMPC, indicating that dynamics near the headgroup regions in the presence of Chol is smallest for the saturated membrane and largest for the polyunsaturated membrane. Even in the presence of Chol, membranes with shorter and saturated acyl chains (Chol/DMPC) have lower mobility parameters compared to a membrane having longer acyl chains with one chain being monounsaturated (Chol/SOPC). The mobility parameters have a statistically significant difference with a p-value ≤ 0.05 for all the Chol-containing membranes except for the Chol/DOPC and Chol/PAPC membranes. Interestingly, the trends of K_a for Chol-containing membranes (Figure 21) are the same as the reverse trends of the mobility parameter (Figure 22), indicating that the less mobile membranes near the headgroup regions have high K_a, like Chol-free membranes discussed above. No significant difference between the mobility parameter of Chol/PAPC and Chol/DOPC membranes was observed, indicating that DOPC with one double bond on each acyl chain and PAPC with one acyl chain saturated and another acyl chain with four double bonds have a similar effect on the dynamics near the headgroup regions of membranes with Chol. Mobility parameters decrease with an increase in α-crystallin concentration for Chol/DMPC and Chol/SOPC membranes (Figure 22 A,B), unlike for Chol/DOPC and Chol/PAPC membranes (Figure 22 C,D). These results show that Chol modulates the mobility parameter of saturated, monounsaturated, and polyunsaturated membranes with increased α-crystallin concentration differently. The decrease in the mobility parameter of Chol/DMPC and Chol/SOPC membranes with the α-crystallin association is not as pronounced as for the same membranes without Chol, indicating that

Chol decreases the capacity of α-crystallin to decrease the mobility parameter. As expected, the mobility parameter of Chol/DOPC and Chol/PAPC membranes do not significantly change with an increase in α-crystallin concentration (Figure 22 C,D). This is because there is no association or minimal association of α-crystallin with these membranes, as seen from the MSO versus α-crystallin concentration data shown in Figure 20 C,D. Previously, we investigated the α-crystallin association with Chol/POPC, Chol/POPS, and Chol/POPE membranes with the same acyl chain length and degree of unsaturation but different headgroups and found that the effect of Chol on modulating the mobility parameter of membranes significantly depends on the lipid headgroup type.[104] The results reported in Figure 22 suggest the synergistic effect of acyl chain length and degree of unsaturation and Chol modulate the membrane dynamics near the headgroup regions with the α-crystallin association. The association of α-crystallin with vesicles made of bovine lens-lipid was investigated previously using fluorophore NBD-PE, which resides near the membrane surface, and found that headgroup mobility of the membrane decreases with the α-crystallin association[92], as reported in this study.

Maximum Splitting of Saturated, Monounsaturated, and Polyunsaturated Membranes with the α-Crystallin Association

The maximum splitting measured from the EPR spectra of the CSL spin-label located near the membrane surface gives the amplitude of wobbling motion of the long axis of the CSL molecule in the membrane.[103,104,117,118,128] The maximum splitting is related to the order parameter, and the higher value of maximum splitting measured with the CSL spin label in the membrane indicates more membrane order near the headgroup region and vice versa.[103,104,117,118,128] In the absence of Chol and α-crystallin, maximum

splitting followed the trends: DMPC > SOPC > DOPC > PAPC, indicating that the saturated membrane with shorter acyl chains has maximum membrane order near the headgroup regions. The significant decrease in the membrane order near the headgroup regions of polyunsaturated DOPC and PAPC membranes than the saturated DMPC and monounsaturated SOPC membranes suggests a higher degree of acyl chain unsaturation significantly decreases the membrane order near the headgroup region (Figure 23). Interestingly, the trends of K_a of α-crystallin association with the membranes (Figure 21) and the trends of the maximum splitting of the membranes (Figure 23) are the same. With the significant decrease in the membrane order near the headgroup regions of polyunsaturated (DOPC and PAPC) membranes, the K_a also decreases significantly, showing the direct correlation between the membrane order near the headgroup region and the K_a. There is a slight decrease in order near the headgroup region of the PAPC membrane than the DOPC membrane; however, there is no significant difference between the K_a values of these membranes. For all the Chol-free membranes with an increase in α-crystallin concentration, the maximum splitting of membranes does not change significantly (Figure 23), indicating that membranes order near the headgroup does not change significantly with the α-crystallin association. In our previous studies, with an increase in α-crystallin concentration, except for the SM and SM/POPE membranes[103], we observed no significant changes in the maximum splitting of membranes made of individual lipids and two-component lipid mixtures[102,103], Chol containing lipid[104], and Chol-containing four-component lipid mixtures.[105]

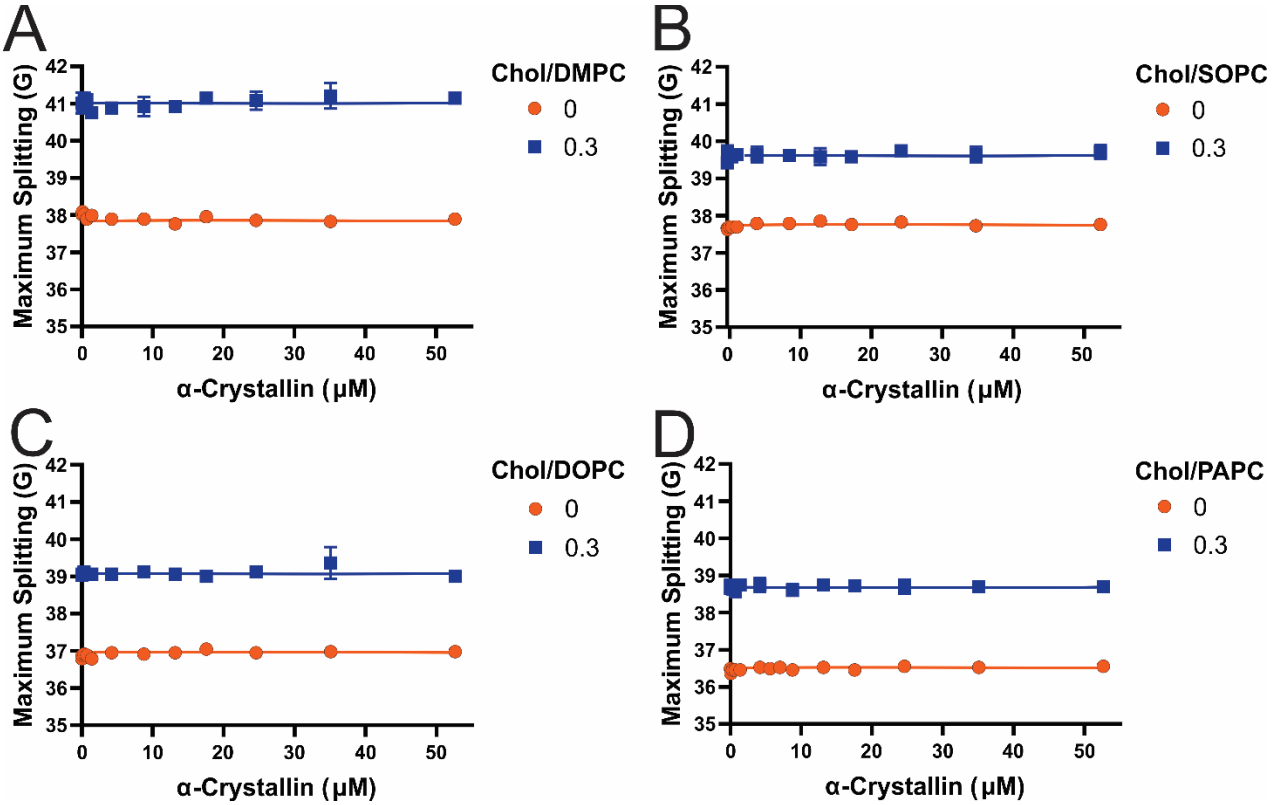

Figure 23 (A–D) Show the profiles of the maximum splitting plotted as a function of α-crystallin concentration for A) Chol/DMPC, B) Chol/SOPC, C) Chol/DOPC, and D) Chol/PAPC membranes, respectively, at Chol and PL mixing ratios of 0 and 0.3. The maximum splitting values are different for different PC membranes, indicating that the order of the membranes near the headgroup regions depends on the acyl chain length and degree of unsaturation of membranes. The trends of the maximum splitting are the same as the trends of the Ka (Figure 21), showing the direct correlation between maximum splitting and the Ka. For all the Chol-free and Chol-containing PC membranes, the maximum splitting does not significantly change with an increase in α-crystallin concentration, representing that the order near the headgroup regions of these membranes does not significantly change with or without α-crystallin association. The addition of Chol increases the maximum splitting of membranes, representing that these membranes become more ordered near the headgroup regions with increased Chol content. The data points are expressed as mean ± standard deviation from three independent experiments, and the solid lines serve as the visual guides.

With the addition of Chol, maximum splitting increases for all the membranes irrespective of the acyl chain length and degree of unsaturation (Figure 23), indicating that the Chol increases the membrane order near the headgroup regions. In the presence of Chol, maximum splitting follows the trends: Chol/DMPC > Chol/SOPC > Chol/DOPC

> Chol/PAPC like Chol-free membrane; however, maximum splitting is significantly higher (i.e., larger membrane order) for saturated (Chol/DMPC) membrane compared to monounsaturated (Chol/SOPC) and polyunsaturated (Chol/DOPC and Chol/PAPC) membranes. The maximum splitting values have a statistically significant difference with a p-value ≤ 0.05 for all the Chol/DMPC, Chol/SOPC, Chol/DOPC, and Chol/PAPC membranes at Chol and PL mixing ratios of 0 and 0.3. Interestingly, the trends of K_a for Chol-containing membranes (Figure 21) are the same as the trends of the maximum splitting (Figure 23), indicating that the membranes with high order near the headgroup regions have high K_a, like Chol-free membranes discussed above. For all the Chol-containing membranes, the maximum splitting does not significantly change with an increase in α-crystallin concentration (Figure 23), indicating that membrane order near the headgroup regions does not significantly change with an increase in α-crystallin concentration.

Human lens lipid composition changes significantly with age, increasing the saturation of acyl chains (i.e., decreasing the double bonds) and a decrease in chain length.[80–84] This may be why the association of α-crystallin with the lens membrane increases with age.[18] It has also been speculated that the lipid order of the membrane increases with age and cataracts[88,89], resulting in a proportional increase in α-crystallin-membrane association.[91]

Surface Hydrophobicity of Saturated, Monounsaturated, and Polyunsaturated Membranes with the α-Crystallin Association

The z-component of the hyperfine interaction tensor (A_z) measured from the EPR spectra of frozen (approximately – 165 °C) samples gives the measure of the hydrophobicity.[105,115–119] The $2A_z$ value measured from the frozen membrane samples using the CSL spin-label gives the measure of hydrophobicity near the headgroup region of the membrane.[105,115,118,119] The decrease in the $2A_z$ value of the CSL spin-label in the membrane means an increase in hydrophobicity (i.e., decrease in polarity) around the nitroxide moiety of CSL.[105,115–119] The nitroxide moiety of CLS resides near the headgroup region of the membrane, as shown in Figure 7. The hydrophobicity near the headgroup regions of membranes slightly increases with the α-crystallin association, as shown in Figure 24A. Previously, we have suggested the hydrophobic interaction of α-crystallin with membranes[103–105], with hydrophobic residues exposed on the surface of α-crystallin associating with membranes.[103,104] It is likely that the α-crystallin, with exposed hydrophobic residues on its surface, associates with the membrane expelling out the water molecules around the polar headgroup regions of the membrane, slightly increasing the hydrophobicity (decreasing the polarity) near the headgroup regions of the membrane. The increase in hydrophobicity is more pronounced for α-crystallin association with the SOPC membrane than with other membranes (Figure 24A), suggesting that acyl chain length and degree of unsaturation modulate hydrophobicity near the headgroup regions of membranes. The hydrophobicity values with and without α-crystallin association with the SOPC membrane have a statistical significance difference with a p-value ≤ 0.05. Other than the SOPC membrane, there is a slight increase in hydrophobicity with an increase in

α-crystallin concentration for other Chol-free membranes; however, the hydrophobicity values have no statistically significant difference with a p-value ≤ 0.05. Chol is a major lens membrane component[61], the addition of which in PL membranes decreased hydrophobicity (Figure 24B) compared to the corresponding Chol-free membranes (Figure 24A), indicating that Chol decreases the hydrophobicity near the headgroup regions of membranes independently of the PL acyl chain length and degree of unsaturation. Chol separates the PL's headgroups allowing water penetration in the region, decreasing hydrophobicity.[119] Our previous study[105] also shows that the addition of Chol decreases hydrophobicity near the headgroup regions of PL membranes. In addition, Chol decreases the mobility parameter, as shown in Figure 22 and our previous studies[104,105], and increases the maximum splitting, as shown in Figure 23 and our previous studies[104,105], representing the fact that membrane regions near the headgroup becomes less mobile and more ordered with the addition of Chol. It has also been reported that Chol modulates nuclear and cortical lens lipids' structural order.[89] Interestingly, the hydrophobicity near the headgroup regions of the membrane decreases with the addition of Chol (Figure 24 A,B), accompanied by the decrease in the MSO (Figure 20) and K_a (Figure 21), suggesting the hydrophobic interaction of α-crystallin with the membrane. Recently, we investigated the association of α-crystallin with Chol/model of human lens-lipid (Chol/MHLL), Chol/model of porcine lens-lipid (Chol/MPLL), and Chol/model of mouse lens-lipid (Chol/MMLL) membranes and discovered a decrease in MSO, K_a, and hydrophobicity with increasing Chol content, implying that α-crystallin interacts with these membranes hydrophobically.[105] Research performed in other laboratories using different approaches (i.e., fluorescence[129],

resonance energy transfer[130], and heat treatment[131]) suggested that α-crystallin interacts with the membrane via hydrophobic interaction. Like Chol-free membranes discussed above in Figure 24A, hydrophobicity near the headgroup region of Chol-containing membranes slightly increases with the α-crystallin (Figure 23B), forming the hydrophobic barrier near the membrane surface. Except for the Chol/SOPC membrane, the hydrophobicity values for the Chol/DMPC, Chol/DOPC, and Chol/PAPC membranes with and without α-crystallin have no statistically significant difference with a p-value ≤ 0.05. Interestingly, the hydrophobicity of Chol/DOPC and Chol/PAPC membranes slightly increases in the presence of α-crystallin, despite no or minimal association of α-crystallin with these membranes (see Figure 20 C,D). We speculate that, even if α-crystallin has no or minimal association with the membrane, water molecules around the headgroup regions of the membrane are likely to be expelled as α-crystallin with exposed hydrophobic sites approaches the membrane, increasing hydrophobicity around the headgroup regions. A similar slight increase in hydrophobicity near the headgroup regions of the Chol/MHLL, Chol/MPLL, and Chol/MMLL membranes was observed (see Figure 25), despite no or minimal association of α-crystallin with these membranes.[105]

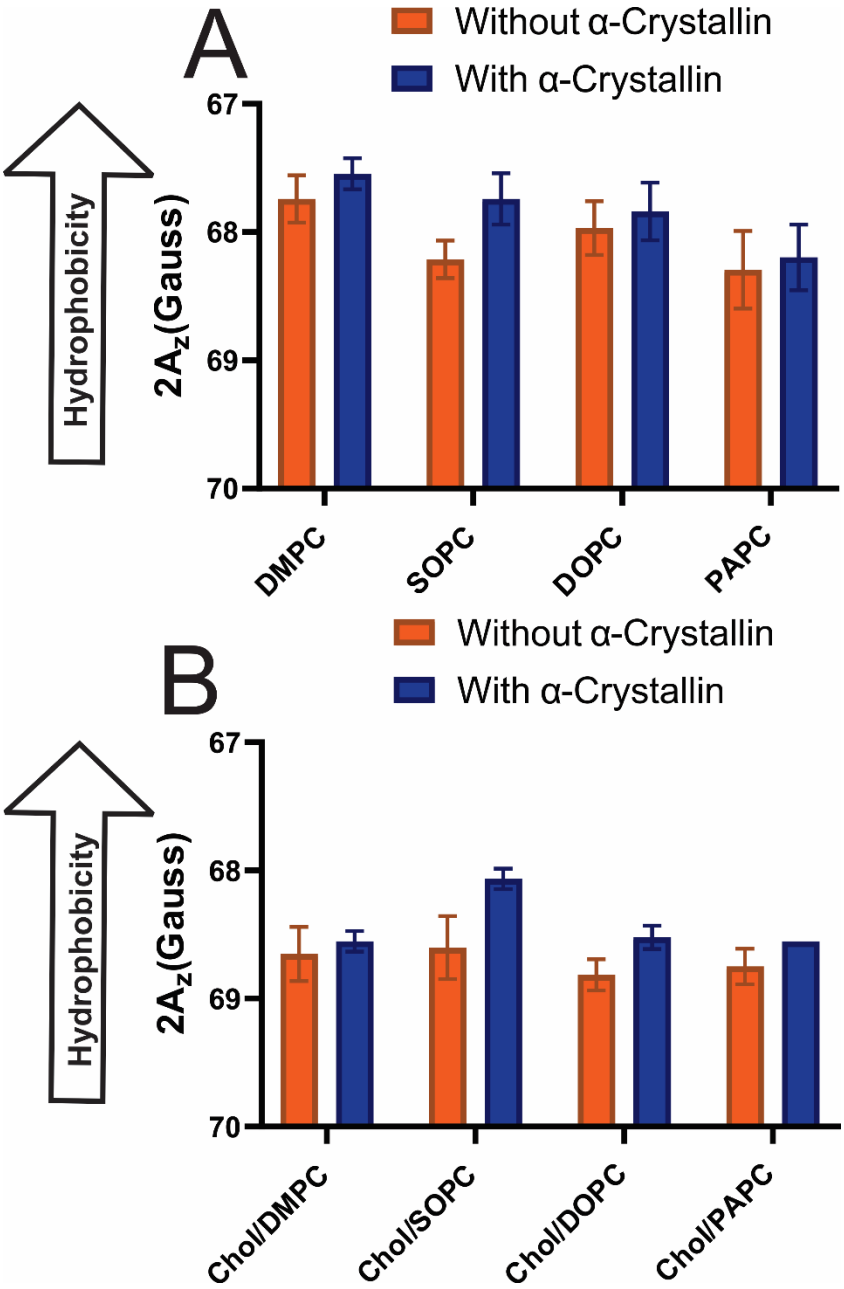

Figure 24 (A-B) Profiles of hydrophobicity (2Az). A) Shows the profiles of hydrophobicity (2Az) with and without α-crystallin for DMPC, SOPC, DOPC, and PAPC membranes; B) shows the profiles of hydrophobicity with and without α-crystallin for Chol/DMPC, Chol/SOPC, Chol/DOPC, and Chol/PAPC membranes with Chol and PL mixing ratio of 0.3. Membrane and α-crystallin membrane samples incubated at 37 °C for 16 h, which are used to measure the MSO shown in Figure 19, are used for hydrophobicity measurements at −165 °C. The 52.6 μM of α-crystallin is used for all the hydrophobicity measurements presented for the α-crystallin membrane samples in Figure 24. Without Chol (Figure 24A), the hydrophobicity for all membranes slightly increases with α-crystallin, representing that the α-crystallin-membrane association slightly increases hydrophobicity (decreases polarity) near the headgroup regions of membranes. Interestingly with

Chol (Figure 24B), the hydrophobicity for all membranes slightly increases with α-crystallin; even no or minimal association of α-crystallin is observed with Chol/DOPC and Chol/PAPC membranes. This suggests that the α-crystallin close to these membrane surfaces expels the water molecules around the headgroup regions, increasing hydrophobicity (decreasing polarity). The data points are expressed as mean ± standard deviation from three independent experiments.

Figure 25A shows that the α-crystallin association with the MHLL, MPLL, and MMLL membranes increases the hydrophobicity near the headgroup regions of these membranes forming the hydrophobic barrier; however, the increase in hydrophobicity depends upon the lipid composition. Hydrophobicity data shown in Figure 25 without α-crystallin were taken from our recent study.[105] The increase in hydrophobicity with α-crystallin association followed the trends: MMLL > MPLL > MHLL. The MMLL, MPLL, and MHLL membranes are made of four major lipids of the eye lens membrane (i.e., SM, POPC, POPS, and POPE). The POPC content in MMLL, MPLL, and MHLL membranes are 46%, 35%, and 11%, respectively and SM content in MMLL, MPLL, and MHLL membranes are 15%, 29%, and 66%, respectively.[105] These data suggest that the increase in hydrophobicity with α-crystallin association increases with an increase in POPC content and decrease in SM content, suggesting that the lipid composition strongly modulates hydrophobicity near the headgroup region of the membrane with the α-crystallin association. For MHLL, MPLL, and MMLL membranes, the hydrophobicity values with and without α-crystallin have a statistically significant difference with a p-value ≤ 0.05. Surprisingly, even with high Chol content (Chol/MHLL mixing ratio of 1.5, and Chol/MPLL and Chol/MMLL mixing ratio of 1), we see a slight increase in hydrophobicity with an increase in α-crystallin concentration (Figure 25B); however, the increase is not as pronounced as for Chol-free MHLL, MPLL, and MMLL membranes (Figure 25A). Except for the Chol/MHLL membrane, the hydrophobicity values for the

Chol/MPLL and Chol/MMLL membranes with and without α-crystallin have no statistically significant difference with a p-value ≤ 0.05. Previously, we found MSO by α-crystallin to be zero or close to zero for Chol/MPLL and Chol/MPLL membranes with a mixing ratio of 1 and Chol/MHLL membrane with a mixing ratio of 1.5, indicating no association or minimal association of α-crystallin with these membranes.[105] As explained above, we speculate that, even if α-crystallin has no or minimal association with these membranes, water molecules around the headgroup regions of membranes are likely to be expelled as α-crystallin with exposed hydrophobic sites approaches membranes, increasing hydrophobicity around the headgroup regions of these membranes.

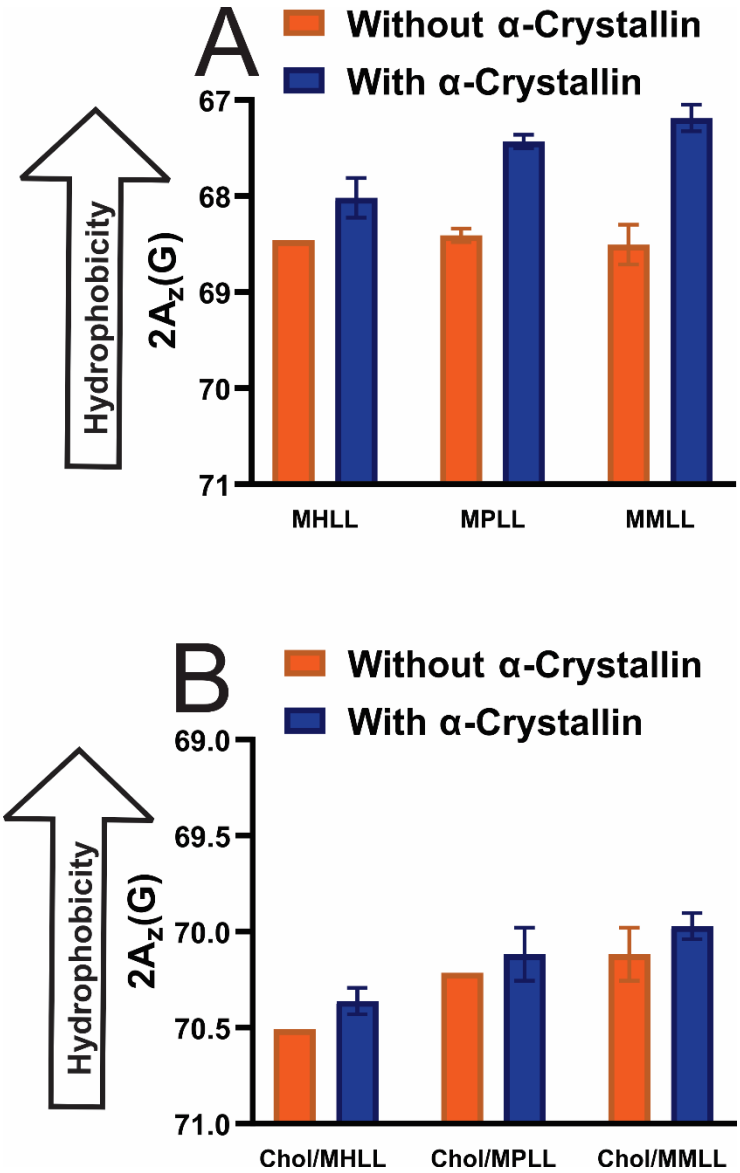

Figure 25 (A-B) Profiles of hydrophobicity (2Az). A) Shows the profiles of hydrophobicity (2Az) with and without α-crystallin for MHLL, MPLL, and MMLL membranes; B) shows the profiles of hydrophobicity with and without α-crystallin for Chol/MHLL, Chol/MPLL, and Chol/MMLL membranes with a Chol/MHLL mixing ratio of 1.5 and Chol/MPLL and Chol/MMLL mixing ratio of 1. Membrane and α-crystallin-membrane samples incubated at 37 °C for 16 h, which are used to measure the MSO shown in Figure 3 of 105, are used for hydrophobicity measurements at -165 °C. The 52.6 μM of α-crystallin is used for all the hydrophobicity measurements presented for the α-crystallin membrane samples in Figure 25. Without Chol (Figure 25A), the hydrophobicity for all membranes increases with α-crystallin, representing that the α-crystallin membrane association increases hydrophobicity (decreases polarity) near the headgroup regions of these membranes. Interestingly, the hydrophobicity for Chol/MHLL, Chol/MPLL, and Chol/MHLL membranes slightly increases with α-crystallin, even no or minimal association of α-crystallin is observed for these membranes (see Figure 3 of ref 105),

suggesting that the α-crystallin close to the membrane surface expels the water molecules around the headgroup regions of membranes, increasing hydrophobicity (decreasing polarity).105 The data points are expressed as mean ± standard deviation from three independent experiments.

The increase in hydrophobicity near the headgroup regions of membranes with α-crystallin association forms the hydrophobic barrier to the transport of polar and ionic molecules. It has been proposed earlier that the α-crystallin associated with lens membrane in the barrier regions after middle age may result in occluding membrane pores and creating an oxidative condition in the lens followed by the development of nuclear cataracts.[94–96] Although the study conducted here does not include membrane proteins, the results indicating the increase in hydrophobicity (i.e., hydrophobic barrier) near the headgroup region of the membrane with α-crystallin association support the barrier hypothesis that α-crystallin association to lens membrane block the transport of metabolites and ions that leads to developing nuclear cataract.[94–96]

CHAPTER 5: CONCLUSIONS AND FUTURE DIRECTIONS

We investigated the association of α-crystallin with Chol/PC membranes of varying chain length and degree of unsaturation and measured the MSO, K_a, and the physical properties (mobility parameter, maximum splitting, and hydrophobicity) of membranes with the α-crystallin association. The MSO increases with an increase in α-crystallin concentration, indicating an increase in the α-crystallin-membrane association. However, the MSO increases rapidly for saturated and monounsaturated membranes than the polyunsaturated membranes. Independently of the acyl chain length and degree of unsaturation, Chol decreases the MSO; however, the decrease in MSO is more significant for polyunsaturated membranes than saturated and monounsaturated membranes. For all membranes with and without Chol, K_a follows the trends, i.e., K_a (14:0–14:0 PC) > K_a (18:0–18:1 PC) > K_a (18:1–18:1 PC) ≈ K_a (16:0–20:4 PC), with the saturated and monounsaturated membranes having significantly higher K_a than the polyunsaturated membranes. The mobility parameter of polyunsaturated membranes is significantly higher than the saturated and monounsaturated membranes, representing that the polyunsaturated membranes are more mobile near the headgroup regions than the saturated and monounsaturated membranes. With increased α-crystallin concentration, the mobility parameter decreases sharply for saturated and monounsaturated membranes than polyunsaturated membranes, indicating that saturated and monounsaturated membranes rapidly become more immobilized near the headgroup regions than polyunsaturated membranes. For all membranes with and without Chol, the maximum

splitting does not significantly change with an increase in α-crystallin concentrations. However, maximum splitting is significantly higher for saturated and monounsaturated membranes than polyunsaturated membranes, indicating that saturated and monounsaturated membranes are more ordered near the headgroup regions than polyunsaturated membranes. Our results directly correlate the mobility and order near the headgroup regions of membranes with the K_a, with the less mobile and more ordered membrane having substantially higher K_a. Furthermore, our results show that the α-crystallin-membrane association increases the hydrophobicity near the headgroup regions of the membrane creating the hydrophobic barrier. The hydrophobic barrier occludes the membrane pores obstructing the transport of polar and ionic molecules, creating an oxidative condition in the lens followed by the nuclear cataract development.[94–96] Although the membranes used in this study do not contain membrane proteins as in the in vivo condition, our study supports the barrier hypothesis that the association of α-crystallin with the lens membrane blocks the transport of ions and metabolites, leading to the development of nuclear cataract.[94–96] The study reported in this thesis shows that the lipid type (acyl chain length and degree of unsaturation) modulates the α-crystallin-membrane association and physical properties (hydrophobicity, mobility parameter, and maximum splitting) of the membrane. Our previous studies[102,103] show that the lipid headgroups modulate the α-crystallin-membrane association and physical properties of the membrane. The combined results of our previous studies[102,103] and the study reported in this thesis suggest that the acyl chain length, degree of acyl chain unsaturation, and lipid headgroups modulate α-crystallin-membrane association and the physical properties of the membrane. Lipids (PLs and sphingolipids) are the primary association sites of α-

crystallin.[74,92,120] The lens lipid composition changes significantly with age, increasing the saturation of acyl chains and decreasing the chain length.[80–84] Moreover, the α-crystallin-membrane association increases with age and cataract formation.[18,91,126] The findings reported in this thesis provide profound insights for understating the role of acyl chain length and degree of unsaturation in modulating the α-crystallin-membrane association and the membrane's physical properties.

My thesis research uses model membranes made of PC with different acyl chain lengths and degrees of unsaturation. PC is the dominant PL in lower-aged animals.[76] In the eye lens membranes, there is a combination of lipids, with a high concentration of Chol and integral membrane proteins. Moreover, lipids and Chol in the lens membranes may be oxidized[20–25], and α-crystallin may have mutations[34–37] and post-translational modifications.[38,39,40–48] Therefore, the association of α-crystallin with eye lens membranes will be affected by the synergistic effect of lipids composition, Chol content, integral membrane proteins, and effects due to such modifications in lipids and α-crystallin. Therefore, further research in this direction is necessary to better understand the α-crystallin-membrane association in native conditions. Since we aimed to understand the role of acyl chain length and degree of unsaturation of PL on the α-crystallin-membrane association, our study clearly shows that the acyl chain length and degree of unsaturation of PL strongly modulate the α-crystallin-membrane association.

Previous studies investigating the association of α-crystallin with membranes used fluorescence approaches[78,106,121,132], in which α-crystallin has a probe. Using a probe in α-crystallin may change its secondary structure. In our EPR spin-labeling approach, we use a spin probe in the membrane, which detects the α-crystallin association with the

membrane. We do not use any probe in the α-crystallin so that its secondary structure does not change. So, one advantage of our α-crystallin-membrane association studies is that the α-crystallin is unmodified and is in the native condition. Another advantage of using the EPR spin-labeling approach is that the experiments are relatively quick and can be performed with minimal amounts of lipids and α-crystallin, such that ~20 μL volume of sample is sufficient for one data point and ~2 mg of lipids and ~0.2 mg of α-crystallin is sufficient to perform one set of experiment.

For the molecular level understanding of α-crystallin-membrane association, MD simulations would be beneficial. α-Crystallin has two subunits αA- and αB-crystallin with 173 and 175 amino acids, respectively, and remains in oligomeric form with about 40 subunits with subunit exchange between oligomers. The MD simulations may be limited due to the enormous size of α-crystallin and membrane system. However, it may be possible to perform MD simulations with single subunit of α-crystallin and the membrane, which would help to understand the molecular level understanding of α-crystallin-membrane association. Moreover, since it is typically simpler for experiments to perform at different experimental conditions and simulations can be corrected (to some extent) by experimental results, synergistic approaches comprising both experiments and MD simulations would be more beneficial to fully understand the α-crystallin-membrane association in molecular level.

My thesis research is among a few studies concerning the role of acyl chain length and degree of unsaturation of PLs in α-crystallin-membrane association. Thus, the topic is still relatively new, and much work remains to be done to fully understand the α-crystallin-membrane association in the eye lens leading to cataract formation. Our

laboratory at Boise State University is making tremendous progress in this direction. Including the thesis research reported here, our previous studies investigating α-crystallin association with individual and two-component PLs and SM membranes[102,103], cholesterol-containing individual PLs and SM membranes[104], and the cholesterol-containing model of human and animal lens lipid membranes[104] clearly show that acyl chain length, degree of acyl chain unsaturation, lipid headgroups, lipid curvature, and lipid and Chol composition strongly modulate α-crystallin association with membranes and the physical properties of membranes. Recently, our laboratory has been studying α-crystallin association with native lens lipid membranes. Also, we are purifying integral membrane proteins, such as MIP26, and optimizing experiments investigating α-crystallin association with membranes containing MIP26.

Moreover, our laboratory aims to purify recombinant αA- and αB-crystallins in the near future. This direction opens new avenues to induce mutations and post-translational modifications to α-crystallin mimicking the modifications in the eye lens, which helps to understand better the role of such modifications in the α-crystallin-membrane interaction and cataract formation. As these studies progress, I hope to collaborate with the lab to further oversee the progress and better understand the role of α-crystallin-membrane association in cataract formation.

REFERENCES

1. Roberts, J. E. (2001). Ocular phototoxicity. *Journal of Photochemistry and Photobiology B: Biology*, *64*(2–3), 136–143. https://doi.org/10.1016/S1011-1344(01)00196-8

2. Roberts, J. E. (2011). *PHOTOBIOLOGY of the HUMAN LENS*. http://photobiology.info/Roberts.html#TOP

3. *How the eye focuses light*. (n.d.). Science Learning Hub. Retrieved August 24, 2022, from https://www.sciencelearn.org.nz/resources/50-how-the-eye-focuses-light

4. Wride, M. A. (2011). Lens fibre cell differentiation and organelle loss: Many paths lead to clarity. *Philosophical Transactions of the Royal Society B: Biological Sciences*, *366*(1568), 1219–1233. https://doi.org/10.1098/rstb.2010.0324

5. Bassnett, S., Shi, Y., & Vrensen, G. F. J. M. (2011). Biological glass: Structural determinants of eye lens transparency. *Philosophical Transactions of the Royal Society B: Biological Sciences*, *366*(1568), 1250–1264. https://doi.org/10.1098/rstb.2010.0302

6. Augusteyn, R. C. (2007). Growth of the human eye lens. *Molecular Vision*, *13*, 252–257.

7. Hejtmancik, J. F., & Shiels, A. (2015). Overview of the Lens. In *Progress in Molecular Biology and Translational Science* (Vol. 134, pp. 119–127). Elsevier. https://doi.org/10.1016/bs.pmbts.2015.04.006

8. Horwitz, J. (2003). Alpha-crystallin. *Experimental Eye Research*, *76*(2), 145–153. https://doi.org/10.1016/s0014-4835(02)00278-6

9. Horwitz, J., Huang, Q. L., Ding, L., & Bova, M. P. (1998). Lens alpha-crystallin: Chaperone-like properties. *Methods in Enzymology*, *290*, 365–383. https://doi.org/10.1016/s0076-6879(98)90032-5

10. Horwitz, J., Bova, M. P., Ding, L. L., Haley, D. A., & Stewart, P. L. (1999). Lens alpha-crystallin: Function and structure. *Eye (London, England)*, *13 (Pt 3b)*, 403–408. https://doi.org/10.1038/eye.1999.114

11. Bloemendal, H., de Jong, W., Jaenicke, R., Lubsen, N. H., Slingsby, C., & Tardieu, A. (2004). Ageing and vision: Structure, stability and function of lens crystallins. *Progress in Biophysics and Molecular Biology*, *86*(3), 407–485. https://doi.org/10.1016/j.pbiomolbio.2003.11.012

12. Horwitz, J. (1992). Alpha-crystallin can function as a molecular chaperone. *Proceedings of the National Academy of Sciences of the United States of America*, *89*(21), 10449–10453. https://www.ncbi.nlm.nih.gov/pmc/articles/PMC50356/

13. Jakob, U., Gaestel, M., Engel, K., & Buchner, J. (1993). Small heat shock proteins are molecular chaperones. *The Journal of Biological Chemistry*, *268*(3), 1517–1520.

14. Lynnerup, N., Kjeldsen, H., Heegaard, S., Jacobsen, C., & Heinemeier, J. (2008). Radiocarbon Dating of the Human Eye Lens Crystallines Reveal Proteins without Carbon Turnover throughout Life. *PLOS ONE*, *3*(1), e1529. https://doi.org/10.1371/journal.pone.0001529

15. Rujoi, M., Jin, J., Borchman, D., Tang, D., & Yappert, M. C. (2003). Isolation and Lipid Characterization of Cholesterol-Enriched Fractions in Cortical and Nuclear Human Lens Fibers. *Investigative Ophthalmology & Visual Science*, *44*(4), 1634–1642. https://doi.org/10.1167/iovs.02-0786

16. Pescosolido, N., Barbato, A., Giannotti, R., Komaiha, C., & Lenarduzzi, F. (2016). Age-related changes in the kinetics of human lenses: Prevention of the cataract. *International Journal of Ophthalmology*. https://doi.org/10.18240/ijo.2016.10.23

17. Borchman, D., & Yappert, M. C. (2010). Lipids and the ocular lens. *Journal of Lipid Research*, *51*(9), 2473–2488. https://doi.org/10.1194/jlr.R004119

18. Timsina, R., & Mainali, L. (2021). Association of Alpha-Crystallin with Fiber Cell Plasma Membrane of the Eye Lens Accompanied by Light Scattering and Cataract Formation. *Membranes*, *11*(6), 447. https://doi.org/10.3390/membranes11060447

19. Khazaeni, L. M. (2022). *Cataract*. MSD. https://www.msdmanuals.com/en-kr/home/eye-disorders/cataract/cataract

20. Bhuyan, K. C., Bhuyan, D. K., & Podos, S. M. (1986). Lipid peroxidation in cataract of the human. *Life Sciences*, *38*(16), 1463–1471. https://doi.org/10.1016/0024-3205(86)90559-x

21. Babizhayev, M. A. (1989). Lipid fluorophores of the human crystalline lens with cataract. *Graefe's Archive for Clinical and Experimental Ophthalmology = Albrecht Von Graefes Archiv Fur Klinische Und Experimentelle Ophthalmologie*, *227*(4), 384–391. https://doi.org/10.1007/BF02169418

22. Borchman, D., Yappert, M. C., Rubini, R. Q., & Paterson, C. A. (1989). Distribution of phospholipid-malondialdehyde-adduct in the human lens. *Current Eye Research*, *8*(9), 939–946.

23. Simonelli, F., Nesti, A., Pensa, M., Romano, L., Savastano, S., Rinaldi, E., & Auricchio, G. (1989). Lipid peroxidation and human cataractogenesis in diabetes and severe myopia. *Experimental Eye Research*, *49*(2), 181–187. https://doi.org/10.1016/0014-4835(89)90088-2

24. Borchman, D., & Yappert, M. C. (1998). Age-related lipid oxidation in human lenses. *Investigative Ophthalmology & Visual Science*, *39*(6), 1053–1058.

25. Girão, H., Mota, M. C., Ramalho, J., & Pereira, P. (1998). Cholesterol oxides accumulate in human cataracts. *Experimental Eye Research*, *66*(5), 645–652. https://doi.org/10.1006/exer.1998.0465

26. Borchman, D. (2020). Lipid Conformational Order and the Etiology of Cataract and Dry Eye. *Journal of Lipid Research*. https://doi.org/10.1194/jlr.tr120000874

27. Borchman, D., Stimmelmayr, R., & George, J. C. (2017). Whales, lifespan, phospholipids, and cataracts. *Journal of Lipid Research*, *58*(12), 2289–2298. https://doi.org/10.1194/jlr.M079368

28. Borchman, D., & Yappert, M. C. (2010). Lipids and the ocular lens. *Journal of Lipid Research*, *51*(9), 2473–2488. https://doi.org/10.1194/jlr.R004119

29. Huang, L., Grami, V., Marrero, Y., Tang, D., Yappert, M. C., Rasi, V., & Borchman, D. (2005). Human Lens Phospholipid Changes with Age and Cataract. *Investigative Ophthalmology & Visual Science*, *46*(5), 1682–1689. https://doi.org/10.1167/iovs.04-1155

30. Mainali, L., Raguz, M., O'Brien, W. J., & Subczynski, W. K. (2017). Changes in the Properties and Organization of Human Lens Lipid Membranes Occurring with Age. *Current Eye Research*, *42*(5), 721–731. https://doi.org/10.1080/02713683.2016.1231325

31. Paterson, C. A., Zeng, J., Husseini, Z., Borchman, D., Delamere, N. A., Garland, D., & Jimenez-Asensio, J. (1997). Calcium ATPase activity and membrane structure in clear and cataractous human lenses. *Current Eye Research*, *16*(4), 333–338. https://doi.org/10.1076/ceyr.16.4.333.10689

32. Truscott, R. J. (2000). Age-related nuclear cataract: A lens transport problem. *Ophthalmic Research*, *32*(5), 185–194. https://doi.org/10.1159/000055612

33. Yappert, M. C., Rujoi, M., Borchman, D., Vorobyov, I., & Estrada, R. (2003). Glycero- versus sphingo-phospholipids: Correlations with human and non-human mammalian lens growth. *Experimental Eye Research*, *76*(6), 725–734. https://doi.org/10.1016/S0014-4835(03)00051-4

34. Andley, U. P. (2009). AA-crystallin R49Cneomutation influences the architecture of lens fiber cell membranes and causes posterior and nuclear cataracts in mice. *BMC Ophthalmology*, *9*(1), 4. https://doi.org/10.1186/1471-2415-9-4

35. Cobb, B. A., & Petrash, J. M. (2000). Structural and Functional Changes in the αA-Crystallin R116C Mutant in Hereditary Cataracts. *Biochemistry*, *39*(51), 15791–15798. https://www.ncbi.nlm.nih.gov/pmc/articles/PMC2902970/

36. Brown, Z., Ponce, A., Lampi, K., Hancock, L., & Takemoto, L. (2007). Differential binding of mutant (R116C) and wildtype alphaA crystallin to actin. *Current Eye Research*, *32*(12), 1051–1054. https://doi.org/10.1080/02713680701769989

37. Grosas, A. B., & Carver, J. A. (2021). Eye Lens Crystallins: Remarkable Long-Lived Proteins. In *Long-lived Proteins in Human Aging and Disease* (pp. 59–96). John Wiley & Sons, Ltd. https://doi.org/10.1002/9783527826759.ch3

38. Kamei, A., Iwase, H., & Masuda, K. (1997). Cleavage of Amino Acid Residue(s) from the N-Terminal Region of αA- and αB-Crystallins in Human Crystalline Lens during Aging. *Biochemical and Biophysical Research Communications*, *231*(2), 373–378. https://doi.org/10.1006/bbrc.1997.6105

39. Kamei, A., Hamaguchi, T., Matsuura, N., & Masuda, K. (2001). Does post-translational modification influence chaperone-like activity of alpha-crystallin? I. Study on phosphorylation. *Biological & Pharmaceutical Bulletin*, *24*(1), 96–99. https://doi.org/10.1248/bpb.24.96

40. Blakytny, R., Carver, J. A., Harding, J. J., Kilby, G. W., & Sheil, M. M. (1997). A spectroscopic study of glycated bovine alpha-crystallin: Investigation of flexibility of the C-terminal extension, chaperone activity and evidence for diglycation. *Biochimica Et Biophysica Acta*, *1343*(2), 299–315. https://doi.org/10.1016/s0167-4838(97)00145-3

41. Bk, D., & Jj, H. (2002). Effects of modifications of alpha-crystallin on its chaperone and other properties. *The Biochemical Journal*, *364*(Pt 3), 711–717. https://doi.org/10.1042/bj20011512

42. van Boekel, M. A., Hoogakker, S. E., Harding, J. J., & de Jong, W. W. (1996). The influence of some post-translational modifications on the chaperone-like activity of alpha-crystallin. *Ophthalmic Research*, *28 Suppl 1*, 32–38. https://doi.org/10.1159/000267940

43. Truscott, R. J. W., & Friedrich, M. G. (2016). The etiology of human age-related cataract. Proteins don't last forever. *Biochimica Et Biophysica Acta*, *1860*(1 Pt B), 192–198. https://doi.org/10.1016/j.bbagen.2015.08.016

44. Chaves, J. M., Srivastava, K., Gupta, R., & Srivastava, O. P. (2008). Structural and functional roles of deamidation and/or truncation of N- or C-termini in human alpha A-crystallin. *Biochemistry*, *47*(38), 10069–10083. https://doi.org/10.1021/bi8001902

45. Takemoto, L. J. (1998). Quantitation of asparagine-101 deamidation from alpha-A crystallin during aging of the human lens. *Current Eye Research*, *17*(3), 247–250. https://doi.org/10.1076/ceyr.17.3.247.5218

46. Miesbauer, L. R., Zhou, X., Yang, Z., Yang, Z., Sun, Y., Smith, D. L., & Smith, J. B. (1994). Post-translational modifications of water-soluble human lens crystallins from young adults. *The Journal of Biological Chemistry*, *269*(17), 12494–12502.

47. Fujii, N., Takata, T., Kim, I., Morishima, K., Inoue, R., Magami, K., Matsubara, T., Sugiyama, M., & Koide, T. (2020). Asp isomerization increases aggregation of α-crystallin and decreases its chaperone activity in human lens of various ages. *Biochimica et Biophysica Acta (BBA) - Proteins and Proteomics*, *1868*(9), 140446. https://doi.org/10.1016/j.bbapap.2020.140446

48. Nagaraj, R. H., Nahomi, R. B., Shanthakumar, S., Linetsky, M., Padmanabha, S., Pasupuleti, N., Wang, B., Santhoshkumar, P., Panda, A. K., & Biswas, A. (2012). Acetylation of αA-crystallin in the human lens: Effects on structure and chaperone function. *Biochimica Et Biophysica Acta*, *1822*(2), 120–129. https://doi.org/10.1016/j.bbadis.2011.11.011

49. Bron, A. J., Vrensen, G. F., Koretz, J., Maraini, G., & Harding, J. J. (2000). The ageing lens. *Ophthalmologica. Journal International D'ophtalmologie. International Journal of Ophthalmology. Zeitschrift Fur Augenheilkunde*, *214*(1), 86–104. https://doi.org/10.1159/000027475

50. Truscott, R. J. W. (2005). Age-related nuclear cataract-oxidation is the key. *Experimental Eye Research*, *80*(5), 709–725. https://doi.org/10.1016/j.exer.2004.12.007

51. Jacob, S. (2013). Ionizing Radiation as a Risk Factor for Cataract: What about Low-Dose Effects? *Journal of Clinical & Experimental Ophthalmology*, *04*(02). https://doi.org/10.4172/2155-9570.S1-005

52. Lipman, R. M., Tripathi, B. J., & Tripathi, R. C. (1988). Cataracts induced by microwave and ionizing radiation. *Survey of Ophthalmology*, *33*(3), 200–210. https://doi.org/10.1016/0039-6257(88)90088-4

53. Uwineza, A., Kalligeraki, A. A., Hamada, N., Jarrin, M., & Quinlan, R. A. (2019). Cataractogenic load – A concept to study the contribution of ionizing radiation to accelerated aging in the eye lens. *Mutation Research/Reviews in Mutation Research*, *779*, 68–81. https://doi.org/10.1016/j.mrrev.2019.02.004

54. Hejtmancik, J. F., & Kantorow, M. (2004). Molecular genetics of age-related cataract. *Experimental Eye Research*, *79*(1), 3–9. https://doi.org/10.1016/j.exer.2004.03.014

55. Shiels, A., & Hejtmancik, J. F. (2007). Genetic Origins of Cataract. *Archives of Ophthalmology*, *125*(2), 165–173. https://doi.org/10.1001/archopht.125.2.165

56. Khatry, S. K., Lewis, A. E., Schein, O. D., Thapa, M. D., Pradhan, E. K., & Katz, J. (2004). The epidemiology of ocular trauma in rural Nepal. *The British Journal of Ophthalmology*, *88*(4), 456–460. https://doi.org/10.1136/bjo.2003.030700

57. Négrel, A.-D., & Thylefors, B. (1998). The global impact of eye injuries. *Ophthalmic Epidemiology*, *5*(3), 143–169. https://doi.org/10.1076/opep.5.3.143.8364

58. Klein, R., & Klein, B. E. (1997). Diabetic eye disease. *The Lancet*, *350*(9072), 197–204. https://doi.org/10.1016/S0140-6736(97)04195-0

59. Pollreisz, A., & Schmidt-Erfurth, U. (2010). *Diabetic Cataract—Pathogenesis, Epidemiology and Treatment* [Review Article]. Journal of Ophthalmology; Hindawi. https://doi.org/10.1155/2010/608751

60. Bassnett, S., Shi, Y., & Vrensen, G. F. J. M. (2011). Biological glass: Structural determinants of eye lens transparency. *Philosophical Transactions of the Royal Society B: Biological Sciences*, *366*(1568), 1250–1264. https://doi.org/10.1098/rstb.2010.0302

61. Borchman, D., Delamere, N. A., McCauley, L. A., & Paterson, C. A. (1989). *STUDIES ON THE DISTRIBUTION OF CHOLESTEROL, PHOSPHOLIPID, AND PROTEIN IN THE HUMAN AND BOVINE LENS*. 24.

62. Cooper, G. M. (2000). *The Cell: A Molecular Approach* (2nd Edition). Sinauer Associates. https://www.ncbi.nlm.nih.gov/books/NBK9839/

63. Kar, R., Batra, N., Riquelme, M. A., & Jiang, J. X. (2012). Biological role of connexin intercellular channels and hemichannels. *Archives of Biochemistry and Biophysics*, *524*(1), 2–15. https://doi.org/10.1016/j.abb.2012.03.008

64. Cenedella, R. J., & Fleschner, C. R. (1992). Selective association of crystallins with lens "native" membrane during dynamic cataractogenesis. *Current Eye Research*, *11*(8), 801–815. https://doi.org/10.3109/02713689209000753

65. Chandrasekher, G., & Cenedella, R. J. (1995). Protein associated with human lens "native" membrane during aging and cataract formation. *Experimental Eye Research*, *60*(6), 707–717. https://doi.org/10.1016/s0014-4835(05)80012-0

66. Fu, S. C., Su, S. W., Wagner, B. J., & Hart, R. (1984). Characterization of lens proteins. IV. Analysis of soluble high molecular weight protein aggregates in human lenses. *Experimental Eye Research*, *38*(5), 485–495. https://doi.org/10.1016/0014-4835(84)90126-x

67. Lampi, K. J., Ma, Z., Hanson, S. R., Azuma, M., Shih, M., Shearer, T. R., Smith, D. L., Smith, J. B., & David, L. L. (1998). Age-related changes in human lens crystallins identified by two-dimensional electrophoresis and mass spectrometry. *Experimental Eye Research*, *67*(1), 31–43. https://doi.org/10.1006/exer.1998.0481

68. Ma, Z., Hanson, S. R., Lampi, K. J., David, L. L., Smith, D. L., & Smith, J. B. (1998). Age-related changes in human lens crystallins identified by HPLC and mass spectrometry. *Experimental Eye Research*, *67*(1), 21–30. https://doi.org/10.1006/exer.1998.0482

69. Spector, A. (1984). The search for a solution to senile cataracts. Proctor lecture. *Investigative Ophthalmology & Visual Science*, *25*(2), 130–146. http://iovs.arvojournals.org/article.aspx?articleid=2176809

70. Srivastava, O. P., Srivastava, K., & Silney, C. (1996). Levels of crystallin fragments and identification of their origin in water soluble high molecular weight (HMW) proteins of human lenses. *Current Eye Research*, *15*(5), 511–520. https://doi.org/10.3109/02713689609000762

71. Friedrich, M. G., & Truscott, R. J. W. (2010). Large-scale binding of α-crystallin to cell membranes of aged normal human lenses: A phenomenon that can be induced by mild thermal stress. *Investigative Ophthalmology & Visual Science*, *51*(10), 5145–5152. https://doi.org/10.1167/iovs.10-5261

72. Datiles, M. B., Ansari, R. R., Yoshida, J., Brown, H., Zambrano, A. I., Tian, J., Vitale, S., Zigler, J. S., Ferris, F. L., West, S. K., & Stark, W. J. (2016). Longitudinal Study of Age Related Cataract Using Dynamic Light Scattering: Loss of α-crystallin Leads to Nuclear Cataract Development. *Ophthalmology*, *123*(2), 248–254. https://doi.org/10.1016/j.ophtha.2015.10.007

73. Borchman, D., & Tang, D. (1996). Binding capacity of alpha-crystallin to bovine lens lipids. *Experimental Eye Research*, *63*(4), 407–410. https://doi.org/10.1006/exer.1996.0130

74. Chandrasekher, G., & Cenedella, R. J. (1997). Properties of alpha-crystallin bound to lens membrane: Probing organization at the membrane surface. *Experimental Eye Research*, *64*(3), 423–430. https://doi.org/10.1006/exer.1996.0228

75. Ifeanyi, F., & Takemoto, L. (1991). Interaction of lens crystallins with lipid vesicles. *Experimental Eye Research*, *52*(5), 535–538. https://doi.org/10.1016/0014-4835(91)90054-i

76. Deeley, J. M., Mitchell, T. W., Wei, X., Korth, J., Nealon, J. R., Blanksby, S. J., & Truscott, R. J. W. (2008). Human lens lipids differ markedly from those of commonly used experimental animals. *Biochimica et Biophysica Acta (BBA) - Molecular and Cell Biology of Lipids*, *1781*(6), 288–298. https://doi.org/10.1016/j.bbalip.2008.04.002

77. Borchman, D., Byrdwell, W. C., & Yappert, M. C. (1994). Regional and age-dependent differences in the phospholipid composition of human lens membranes. *Investigative Ophthalmology & Visual Science*, *35*(11), 3938–3942. https://iovs.arvojournals.org/article.aspx?articleid=2179507

78. Cobb, B. A., & Petrash, J. M. (2002). Factors influencing α-crystallin association with phospholipid vesicles. *Molecular Vision*, *8*, 85–93. https://www.ncbi.nlm.nih.gov/pmc/articles/PMC2902965/

79. Yappert, M. C., & Borchman, D. (2004). Sphingolipids in human lens membranes: An update on their composition and possible biological implications. *Chemistry and Physics of Lipids*, *129*(1), 1–20. https://doi.org/10.1016/j.chemphyslip.2003.12.003

80. Borchman, D., CraigByrdwell, W., & Yappert, M. C. (1994). *Regional and Age-Dependent Differences in the Phospholipid Composition of Human Lens Membranes*. 5.

81. Deeley, J. M., Mitchell, T. W., Wei, X., Korth, J., Nealon, J. R., Blanksby, S. J., & Truscott, R. J. W. (2008). Human lens lipids differ markedly from those of commonly used experimental animals. *Biochimica et Biophysica Acta (BBA) - Molecular and Cell Biology of Lipids*, *1781*(6–7), 288–298. https://doi.org/10.1016/j.bbalip.2008.04.002

82. Yappert, M. C., Rujoi, M., Borchman, D., Vorobyov, I., & Estrada, R. (2003). Glycero- versus sphingo-phospholipids: Correlations with human and non-human mammalian lens growth. *Experimental Eye Research*, *76*(6), 725–734. https://doi.org/10.1016/S0014-4835(03)00051-4

83. Yappert, M. C., & Borchman, D. (2004). Sphingolipids in human lens membranes: An update on their composition and possible biological implications. *Chemistry and Physics of Lipids*, *129*(1), 1–20. https://doi.org/10.1016/j.chemphyslip.2003.12.003

84. Cobb, B. A., & Petrash, J. M. (2010). *Factors influencing α-crystallin association with phospholipid vesicles*. 19.

85. Mainali, L., Raguz, M., O'Brien, W. J., & Subczynski, W. K. (2013). Properties of membranes derived from the total lipids extracted from the human lens cortex and nucleus. *Biochimica et Biophysica Acta (BBA) - Biomembranes*, *1828*(6), 1432–1440. https://doi.org/10.1016/j.bbamem.2013.02.006

86. Mainali, L., Raguz, M., O'Brien, W. J., & Subczynski, W. K. (2015). Properties of membranes derived from the total lipids extracted from clear and cataractous lenses of 61–70-year-old human donors. *European Biophysics Journal*, *44*(1–2), 91–102. https://doi.org/10.1007/s00249-014-1004-7

87. Mainali, L., Raguz, M., O'Brien, W. J., & Subczynski, W. K. (2017). Changes in the Properties and Organization of Human Lens Lipid Membranes Occurring with Age. *Current Eye Research*, *42*(5), 721–731. https://doi.org/10.1080/02713683.2016.1231325

88. Borchman, D., Ozaki, Y., Lamba, O. P., Byrdwell, W. C., Czarnecki, M. A., & Yappert, M. C. (1995). Structural characterization of clear human lens lipid membranes by near-infrared Fourier transform Raman spectroscopy. *Current Eye Research*, *14*(6), 511–515. https://doi.org/10.3109/02713689509003763

89. Borchman, D., Cenedella, R. J., & Lamba, O. P. (1996). Role of Cholesterol in the Structural Order of Lens Membrane Lipids. *Experimental Eye Research*, *62*(2), 191–198. https://doi.org/10.1006/exer.1996.0023

90. Paterson, C. A., Zeng, J., Husseini, Z., Borchman, D., Delamere, N. A., Garland, D., & Jimenez-Asensio, J. (1997). Calcium ATPase activity and membrane structure in clear and cataractous human lenses. *Current Eye Research*, *16*(4), 333–338. https://doi.org/10.1076/ceyr.16.4.333.10689

91. Tang, D., Borchman, D., Yappert, M. C., & Cenedella, R. J. (1998). Influence of Cholesterol on the Interaction of α-Crystallin with Phospholipids. *Experimental Eye Research*, *66*(5), 559–567. https://doi.org/10.1006/exer.1997.0467

92. Borchman, D., & Tang, D. (1996). Binding Capacity of α-Crystallin to Bovine Lens Lipids. *Experimental Eye Research*, *63*(4), 407–410. https://doi.org/10.1006/exer.1996.0130

93. Zhu, X., Gaus, K., Lu, Y., Magenau, A., Truscott, R. J. W., & Mitchell, T. W. (2010). α- and β-Crystallins Modulate the Head Group Order of Human Lens Membranes during Aging. *Investigative Opthalmology & Visual Science*, *51*(10), 5162. https://doi.org/10.1167/iovs.09-4947

94. Friedrich, M. G., & Truscott, R. J. W. (2009). Membrane Association of Proteins in the Aging Human Lens: Profound Changes Take Place in the Fifth Decade of Life. *Investigative Opthalmology & Visual Science*, *50*(10), 4786. https://doi.org/10.1167/iovs.09-3588

95. Friedrich, M. G., & Truscott, R. J. W. (2010). *Large-Scale Binding of ⎵-Crystallin to Cell Membranes of Aged Normal Human Lenses: A Phenomenon That Can Be Induced by Mild Thermal Stress*. *51*(10), 8.

96. Truscott, R. J. W. (2005). Age-related nuclear cataract—Oxidation is the key. *Experimental Eye Research*, *80*(5), 709–725. https://doi.org/10.1016/j.exer.2004.12.007

97. Gonen, T., Cheng, Y., Sliz, P., Hiroaki, Y., Fujiyoshi, Y., Harrison, S. C., & Walz, T. (2005). Lipid–protein interactions in double-layered two-dimensional AQP0 crystals. *Nature*, *438*(7068), 633–638. https://doi.org/10.1038/nature04321

98. Reichow, S. L., & Gonen, T. (2009). Lipid–protein interactions probed by electron crystallography. *Current Opinion in Structural Biology*, *19*(5), 560–565. https://doi.org/10.1016/j.sbi.2009.07.012

99. Delamere, N. A., & Tamiya, S. (2009). Lens ion transport: From basic concepts to regulation of Na,K-ATPase activity. *Experimental Eye Research*, *88*(2), 140–143. https://doi.org/10.1016/j.exer.2008.05.005

100. Rhodes, J. D., & Sanderson, J. (2009). The mechanisms of calcium homeostasis and signalling in the lens. *Experimental Eye Research*, *88*(2), 226–234. https://doi.org/10.1016/j.exer.2008.10.025

101. Srivastava, O., Srivastava, K., Joseph, R., & Wilson, L. (2020). Increased Association of Deamidated αA-N101D with Lens membrane of transgenic αAN101D vs. wild type αA mice: Potential effects on intracellular ionic imbalance and membrane disorganization. *BMC Ophthalmology*, *20*(1), 484. https://doi.org/10.1186/s12886-020-01734-0

102. Mainali, L., O'Brien, W. J., & Timsina, R. (2021). Interaction of Alpha-Crystallin with Phospholipid Membranes. *Current Eye Research*, *46*(2), 185–194. https://doi.org/10.1080/02713683.2020.1786131

103. Timsina, R., Khadka, N. K., Maldonado, D., & Mainali, L. (2021). Interaction of alpha-crystallin with four major phospholipids of eye lens membranes. *Experimental Eye Research*, *202*, 108337. https://doi.org/10.1016/j.exer.2020.108337

104. Timsina, R., Trossi-Torres, G., O'Dell, M., Khadka, N. K., & Mainali, L. (2021). Cholesterol and cholesterol bilayer domains inhibit binding of alpha-crystallin to the membranes made of the major phospholipids of eye lens fiber cell plasma membranes. *Experimental Eye Research*, *206*, 108544. https://doi.org/10.1016/j.exer.2021.108544

105. Timsina, R., Trossi-Torres, G., Thieme, J., O'Dell, M., Khadka, N. K., & Mainali, L. (2022). Alpha-Crystallin Association with the Model of Human and Animal Eye Lens-Lipid Membranes is Modulated by Surface Hydrophobicity of Membranes. *Current Eye Research*, 1–19. https://doi.org/10.1080/02713683.2022.2040539

106. Cobb, B. A., & Petrash, J. M. (2000). Structural and Functional Changes in the αA-Crystallin R116C Mutant in Hereditary Cataracts. *Biochemistry*, *39*(51), 15791–15798. https://doi.org/10.1021/bi001453j

107. Buboltz, J. T. (2009). A more efficient device for preparing model-membrane liposomes by the rapid solvent exchange method. *Review of Scientific Instruments*, *80*(12), 124301. https://doi.org/10.1063/1.3264073

108. Mainali, L., Raguz, M., & Subczynski, W. K. (2013). Formation of Cholesterol Bilayer Domains Precedes Formation of Cholesterol Crystals in Cholesterol/Dimyristoylphosphatidylcholine Membranes: EPR and DSC Studies. *The Journal of Physical Chemistry B*, *117*(30), 8994–9003. https://doi.org/10.1021/jp402394m

109. Buboltz, J. T., & Feigenson, G. W. (1999). A novel strategy for the preparation of liposomes: Rapid solvent exchange. *Biochimica et Biophysica Acta (BBA) - Biomembranes*, *1417*(2), 232–245. https://doi.org/10.1016/S0005-2736(99)00006-1

110. Huang, J., Buboltz, J. T., & Feigenson, G. W. (1999). Maximum solubility of cholesterol in phosphatidylcholine and phosphatidylethanolamine bilayers. *Biochimica et Biophysica Acta (BBA) - Biomembranes*, *1417*(1), 89–100. https://doi.org/10.1016/S0005-2736(98)00260-0

111. Zareba, M., Widomska, J., Burke, J. M., & Subczynski, W. K. (2016). Nitroxide free radicals protect macular carotenoids against chemical destruction (bleaching) during lipid peroxidation. *Free Radical Biology and Medicine*, *101*, 446–454. https://doi.org/10.1016/j.freeradbiomed.2016.11.012

112. Kudrle, V., Vašina, P., Tálský, A., Mrázková, M., Štec, O., & Janča, J. (2010). Plasma diagnostics using electron paramagnetic resonance. *Journal of Physics D: Applied Physics*, *43*(12), 124020. https://doi.org/10.1088/0022-3727/43/12/124020

113. Sahu, I. D., & Lorigan, G. A. (2020). Electron Paramagnetic Resonance as a Tool for Studying Membrane Proteins. *Biomolecules*, *10*(5), 763. https://doi.org/10.3390/biom10050763

114. Chechik, V., Carter, E., & Murphy, D. (2016). *Electron Paramagnetic Resonance*. Oxford Chemistry Primers.

115. Mainali, L., Raguz, M., & Subczynski, W. K. (2011). Phase-Separation and Domain-Formation in Cholesterol-Sphingomyelin Mixture: Pulse-EPR Oxygen Probing. *Biophysical Journal*, *101*(4), 837–846. https://doi.org/10.1016/j.bpj.2011.07.014

116. Mainali, L., Raguz, M., O'Brien, W. J., & Subczynski, W. K. (2012). Properties of fiber cell plasma membranes isolated from the cortex and nucleus of the porcine eye lens. *Experimental Eye Research*, *97*(1), 117–129. https://doi.org/10.1016/j.exer.2012.01.012

117. Mainali, L., Raguz, M., & Subczynski, W. K. (2012). Phases and domains in sphingomyelin–cholesterol membranes: Structure and properties using EPR spin-labeling methods. *European Biophysics Journal*, *41*(2), 147–159. https://doi.org/10.1007/s00249-011-0766-4

118. Raguz, M., Mainali, L., Widomska, J., & Subczynski, W. K. (2011). Using spin-label electron paramagnetic resonance (EPR) to discriminate and characterize the cholesterol bilayer domain. *Chemistry and Physics of Lipids*, *164*(8), 819–829. https://doi.org/10.1016/j.chemphyslip.2011.08.001

119. Subczynski, W. K., Wisniewska, A., Yin, J.-J., Hyde, J. S., & Kusumi, A. (1994). Hydrophobic Barriers of Lipid Bilayer Membranes Formed by Reduction of Water Penetration by Alkyl Chain Unsaturation and Cholesterol. *Biochemistry*, *33*(24), 7670–7681. https://doi.org/10.1021/bi00190a022

120. Ifeanyi, F., & Takemoto, L. (1991). Interaction of lens crystallins with lipid vesicles. *Experimental Eye Research*, *52*(5), 535–538. https://doi.org/10.1016/0014-4835(91)90054-I

121. Tang, D., & Borchman, D. (1998). Temperature Induced Structural Changes ofβ-Crystallin and Sphingomyelin Binding. *Experimental Eye Research*, *67*(1), 113–118. https://doi.org/10.1006/exer.1998.0497

122. Mulders, J. W. M., Stokkermans, J., Leunissen, J. A. M., Benedetti, E. L., Bloemendal, H., & Jong, W. W. (1985). Interaction of alpha-crystallin with lens plasma membranes. Affinity for MP26. *European Journal of Biochemistry*, *152*(3), 721–728. https://doi.org/10.1111/j.1432-1033.1985.tb09253.x

123. Tsvetkova, N. M., Horváth, I., Török, Z., Wolkers, W. F., Balogi, Z., Shigapova, N., Crowe, L. M., Tablin, F., Vierling, E., Crowe, J. H., & Vígh, L. (2002). Small heat-shock proteins regulate membrane lipid polymorphism. *Proceedings of the National Academy of Sciences*, *99*(21), 13504–13509. https://doi.org/10.1073/pnas.192468399

124. Boyle, D. L., & Takemoto, L. (1996). EM immunolocalization of α-crystallins: Association with the plasma membrane from normal and cataractous human lenses. *Current Eye Research*, *15*(5), 577–582. https://doi.org/10.3109/02713689609000769

125. Chandrasekher, G., & Cenedella, R. J. (1995). Protein associated with human lens 'native' membrane during aging and cataract formation. *Experimental Eye Research*, *60*(6), 707–717. https://doi.org/10.1016/S0014-4835(05)80012-0

126. Datiles, M. B., Ansari, R. R., Yoshida, J., Brown, H., Zambrano, A. I., Tian, J., Vitale, S., Zigler, J. S., Ferris, F. L., West, S. K., & Stark, W. J. (2016). Longitudinal Study of Age-Related Cataract Using Dynamic Light Scattering. *Ophthalmology*, *123*(2), 248–254. https://doi.org/10.1016/j.ophtha.2015.10.007

127. Schreier, S., Polnaszek, C. F., & Smith, I. C. P. (1978). Spin labels in membranes problems in practice. *Biochimica et Biophysica Acta (BBA) - Reviews on Biomembranes*, *515*(4), 395–436. https://doi.org/10.1016/0304-4157(78)90011-4

128. Kusumi, A., Subczynski, W. K., Pasenkiewicz-Gierula, M., Hyde, J. S., & Merkle, H. (1986). Spin-label studies on phosphatidylcholine-cholesterol membranes: Effects of alkyl chain length and unsaturation in the fluid phase. *Biochimica et Biophysica Acta (BBA) - Biomembranes*, *854*(2), 307–317. https://doi.org/10.1016/0005-2736(86)90124-0

129. Cobb, B. A., & Petrash, J. M. (2010). *Characterization of α-Crystallin-Plasma Membrane Binding*. 24.

130. Tang, D., Borchman, D., & Yappert, M. C. (1999). Alpha-Crystallin/Lens Lipid Interactions Using Resonance Energy Transfer. *Ophthalmic Research*, *31*(6), 452–462. https://doi.org/10.1159/000055571

131. Tjondro, H. C., Xi, Y.-B., Chen, X.-J., Su, J.-T., & Yan, Y.-B. (2016). Membrane insertion of αA-crystallin is oligomer-size dependent. *Biochemical and Biophysical Research Communications*, *473*(1), 1–7. https://doi.org/10.1016/j.bbrc.2016.03.033

132. Cobb, B. A., & Petrash, J. M. (2000). Characterization of alpha-crystallin-plasma membrane binding. *The Journal of Biological Chemistry*, *275*(9), 6664–6672. https://doi.org/10.1074/jbc.275.9.6664